ELSEVIER

Wave Motion 20 (1994) 57–82

WAVE MOTION

Elastic wave up/down decomposition in inhomogeneous and anisotropic media: an operator approach and its approximations

Maarten V. de Hoop [a,1], Adrianus T. de Hoop [b]

[a] *Schlumberger Cambridge Research, High Cross, Madingley Road, Cambridge CB3 0EL, UK*

[b] *Laboratory of Electromagnetic Research, Faculty of Electrical Engineering, Delft University of Technology, P.O. Box 5031, 2600 GA Delft, the Netherlands*

Received 2 January 1994; revised 16 March 1994

Abstract

A structural operator approach to the up/down decomposition of elastic waves in inhomogeneous and anisotropic media is presented. First, the up/down decomposition is carried out; next, a decomposition of the wave field into its polarization constituents is worked out. The procedure is discussed in detail for the class of orthorhombic media and includes lateral variations. The high-frequency approximation to the operator approach is shown to be amenable to matrix manipulations in the horizontal Fourier transform domain. Two-level parabolic approximations are carried out to find sparse matrix (finite-difference) representations of the relevant operators. Finally, the space–time peculiarities and artifacts associated with the parabolic approximation to the particle velocity of the wave motion generated by a point force in a homogeneous and isotropic solid are discussed.

1. Introduction

For the next few years, research in seismic prospecting methods is expected to concentrate on the feasibility of: (a) three-dimensional, three-component data acquisition and processing, (b) incorporation of anisotropy in the analysis, (c) incorporation of lateral variations in the subsurface configuration.

From a mathematical point of view, the problem of reconstructing the subsurface structure of the earth is an inverse scattering problem. Due to the enormous amount of data involved, the degree of complexity of the problem, and the amount of detail with which the local constituency of, for example, a reservoir is needed, the application of the basic procedures of inverse scattering as they could, for example, be based on reciprocity [1], is out of the question, even with present-day computational facilities. Therefore, approximations, possibly adjusted to a particular feature one is interested in, are a necessity. As a matter of fact, both the forward modeling and the inversion procedures have to be carried out computationally. In this respect it would be advantageous if, at least partially, the presently available software, including the established approximations

[1] Corresponding author, telephone (+44-223) 325 311, fax (44-223) 61473.

SSDI 0165-2125(94)00015-W

to, for example, wave extrapolation operators such as the parabolic approximation [2], could also be used under the more complicated circumstances. With this perspective in mind, the present study, which is focused on the forward modeling, has been set up.

A large class of wave equation based seismic migration/inversion schemes in use (see, e.g., Ref. [3]) is based on the decomposition into up- and downgoing waves. With this in mind, we have developed an operator formalism for the up/down decomposition of elastic waves in fully inhomogeneous, anisotropic elastic solids, where up/down is defined with respect to a given direction of preference. In practice, the latter direction is to be chosen in the direction of most rapid variation of the medium parameters ('depth' direction, but this may be inclined with respect to the vertical direction), while in the plane perpendicular to this ('lateral' plane) the variations in the medium parameters are assumed to be less rapid. It is argued that this up/down decomposition be carried out prior to a decomposition into polarization states (like P-, SV- and SH-waves in a configuration consisting of mutually parallel, homogeneous, isotropic layers). The interaction between up- and downgoing waves due to inhomogeneities is then described by a kind of reflectivity operator as in the Bremmer coupling series [4]. The terms in this Bremmer coupling series separates 'up' and 'down' only, and hence not 'left' and 'right' (in the lateral sense). A full separation is only achieved in the high frequency approximation; then the coupling in the sense of the Bremmer series is accounted for by the generalized Born method [5].

A full elastic wave up/down decomposition scheme is set up for arbitrarily inhomogeneous media that are anisotropic with up/down symmetry, in particular with orthorhombic symmetry; the planes of symmetry are assumed to be fixed. For a number of mathematical details, such as the existence proofs for, and the construction of, the pertaining pseudo-differential operators, the reader is referred to Ref. [4]. In the present paper, the attention is focused on the main line of thought.

To detect the presence of anisotropy it is advantageous to extract the signals corresponding to particular polarization states. Therefore, after the decomposition into up- and downgoing waves has been carried out, the operator formalism for the decomposition into polarization states is worked out. In the general case, this decomposition involves the symbol calculus of pseudo-differential operators. The leading term in the high-frequency approximation can, however, be determined analytically with the use of spatial Fourier components in the lateral directions. This term is also the lowest-order term in the expansion of the full symbols in the lateral variations in the medium properties.

Next, we investigate what are the consequences of the parabolic approximation to the wave operators in the preferred direction. This approximation leads to artifacts, which can be misinterpreted if proper care is not taken (see Ref. [6,7] for the analysis of artifacts in the acoustic case). To have at least an indication of what can be expected in the full elastic case, the simple problem of finding the exact space–time wave motion generated by a point force in an unbounded homogeneous, isotropic solid has been studied. For this case, the parabolic approximation is carried out completely along the lines of the earlier developed operator formalism pertinent to the general, laterally varying media. The analysis shows that the corresponding consistent parabolic approximation is not at all trivial and that the results differ from those that would be obtained by applying the parabolic approximation to the standard P- and S-wave Lamé potentials in isotropic solids. This difference is due to the fact that in our analysis the decomposition into up- and downgoing waves is carried out prior to a decomposition into polarization states (P- and S-waves), whereas in the analysis based on the Lamé potentials a decomposition into polarization states (P- and S-waves) is carried out prior to a decomposition into up- and downgoing waves (with a subsequent parabolic approximation to the 'wave extrapolation' operator). In our opinion, our analysis seems to be more fundamental and appropriate for the more complicated phenomena in arbitrarily inhomogeneous and anisotropic media. The occurrence of artifacts and their degree of seriousness are illustrated. To this end, the exact space–time equivalent to the parabolic approximation to this simple problem has been determined with the aid of the modified Cagniard method [8,9], and the two radiation patterns are mutually compared.

As regards the parabolic approximation carried out on the extrapolation operator, a wealth of literature

exists. The most pertinent papers are briefly discussed below. One approach to the parabolic approximation is to transform the relevant wave equations to a moving frame of reference and subsequently separate the slow from the rapid variations. For an almost homogeneous, isotropic solid, Hudson [10,11] derived two simultaneous parabolic theories, one for constituents close to the P waves and one for constituents close to the S waves. An extension of his work can be found in Ref. [12]. A formulation based on the divergence and curl of the particle velocity or displacement fields (which also results in a separation into P and S waves) has been developed by Landers and Claerbout [13]. In their work the coupling between the (perturbed) constituents is assumed to be small. A formulation developed by McCoy [14] does account for this coupling. The differences between the three approaches have been discussed by Wales and McCoy [15] and Wales [16].

Our formulation is developed for anisotropic media (with orthorhombic symmetry) in which three modes of propagation exist. The planes of mirror symmetry are the candidates for the 'lateral' directions. A consistent scheme for parabolic approximations is presented. With it, the three branches of the vertical slowness matrix that has resulted from the prior up/down decomposition are approximated. In this respect it is observed that the order of the parabolic approximation and the order of the singularity of the slowness surface should be compatible. The procedure builds on the work of McCoy [14] and Wapenaar and Berkhout [17], and involves a rearrangement of the 'wave splitting' procedure employed by Corones et al. [18] (see also, Ref. [19]). Results are shown for the cases of a hexagonal solid (solid with TIV symmetry) and an isotropic solid.

In the analysis of acoustic waveguides (as they occur in ocean acoustics), one-way equations can be used to calculate the relevant modal constituents [20,21]. In this case, the preferred direction of propagation is parallel to the interfaces rather than perpendicular to them. This also applies to channel waves occurring, for example, in low wave-speed layers in cross-well experiments.

2. The elastodynamic wave-matrix formalism

We consider linearized elastic waves in an orthorhombic solid occupying some subdomain of three-dimensional space $\mathcal{R}^3$. The point at which the wave motion is observed is specified by the coordinates $\{x_1, x_2, x_3\}$ in a Cartesian reference frame with the origin O and three mutually perpendicular base vectors $\{i_1, i_2, i_3\}$ each of unit length. In the indicated order, the base vectors form a right-handed system. In accordance with geophysical convention, x_3 is taken as the vertical, or depth, coordinate (which increases in the downward direction) leaving x_1, x_2 as the horizontal coordinates. The subscript notation for Cartesian vectors and tensors is employed, and the summation convention applies. Lowercase Greek subscripts are used to indicate the horizontal components of a vector or a tensor in three dimensions. The time coordinate is denoted by t. Differentiation with respect to x_m is denoted by ∂_m; ∂_t represents differentiation with respect to t. The coordinate planes (with as their normals i_1, i_2, i_3) are assumed to be the fixed planes of mirror symmetry in the anisotropy throughout the medium, irrespective of its inhomogeneities.

2.1. The basic equations in the complex-frequency domain

The linearized elastic wave motion in a continuously varying, orthorhombic (fixed axes of symmetry) perfectly elastic solid is characterized by the hyperbolic system of first-order differential equations

$$-\Delta_{kmpq}\partial_m\tau_{pq} + \rho\partial_t v_k = f_k, \tag{1}$$

$$-s_{ijpq}\partial_t\tau_{pq} + \Delta_{ijmr}\partial_m v_r = h_{ij}, \tag{2}$$

where

$$\Delta_{ijpq} = \frac{1}{2}(\delta_{ip}\delta_{jq} + \delta_{iq}\delta_{jp}), \tag{3}$$

and τ_{pq} = stress, v_r = particle velocity, ρ = volume density of mass, s_{ijpq} = compliance, f_k = volume source density of force, $h_{ji} = h_{ij}$ = volume source density of deformation rate, δ_{ip} = Kronecker tensor. It is assumed that s_{ijpq} and ρ are time independent. Through the standard Voigt (cf. Refs. [22,23]) compression of indices: $11 \to 1$, $22 \to 2$, $33 \to 3$, $23, 32 \to 4$, $13, 31 \to 5$ and $12, 21 \to 6$, s_{ijpq} is represented by the 6×6 compliance matrix s_{mn}. (In this process, the elements with the compressed indices 4, 5, 6 are weighted with a factor of 2, e.g., $s_{66} = 4s_{1212}$.) The compliance matrix is simply the inverse of the stiffness matrix c_{mn}. For the assumed symmetry, the non-vanishing elements of the stiffness matrix are $c_{11}, c_{12}, c_{13}, c_{23}, c_{22}, c_{33}, c_{44}, c_{55}, c_{66}$. Assuming that the sources that generate the wave field are switched on at the instant $t = 0$, causality implies that the wave field quantities satisfy the initial conditions

$$\begin{aligned} \tau_{pq}(x_m, t) &= 0 \quad \text{for } t < 0, \\ v_r(x_m, t) &= 0 \quad \text{for } t < 0. \end{aligned} \tag{4}$$

In view of the time invariance of the medium, the causality of the wave motion can be taken into account by carrying out a one-sided Laplace transformation with respect to time, taking the time Laplace-transform parameter s, which in general is complex-valued, to be in the right half $\mathrm{Re}\{s\} > 0$ of the complex s-plane and requiring that the transform-domain wave quantities be bounded functions of position in all space. To show the notation, we give the expression for the particle velocity

$$\hat{v}_r(x_m, s) = \int_{t=0}^{\infty} v_r(x_m, t) \exp(-st)\, \mathrm{d}t. \tag{5}$$

2.2. Scaling of the vertical stress

A decomposition of the elastic equations (1) and (2), and of the stress, into their horizontal and vertical components is carried out. In the equations for the vertical stresses, a scaling is applied. Let the local medium slownesses along the vertical direction be $c_3^{-1} = (\rho/c_{33})^{1/2}$, $c_4^{-1} = (\rho/c_{44})^{1/2}$ and $c_5^{-1} = (\rho/c_{55})^{1/2}$, and let us arrange them in the diagonal matrix

$$C = \begin{pmatrix} \frac{1}{c_5} & 0 & 0 \\ 0 & \frac{1}{c_4} & 0 \\ 0 & 0 & \frac{1}{c_3} \end{pmatrix}. \tag{6}$$

For constructing the one-way wave operator in inhomogeneous media, the traction needs to be normalized with an elastic wave admittance matrix Y, i.e., the traction needs to get the dimension of particle velocity, according to

$$\hat{\tau}'_{i3} = Y_{ir}\, \hat{\tau}_{r3}, \qquad Y = C/\rho, \tag{7}$$

2.3. The reduced equations

Let

$$D_\mu = -\frac{1}{s}\partial_\mu, \quad \mu \in \{1, 2\}, \tag{8}$$

represent the *horizontal slowness* operators. Expressing the horizontal stresses in terms of $\hat{v}_k$ and $\hat{\tau}_{i3}$, and eliminating them from Eqs. (1) and (2), we obtain the scaled reduced hyperbolic system of differential equations

$$\partial_3 \hat{v}_k = -sT_{kr}\hat{v}_r + sC_{kr}\hat{\tau}'_{r3} + \hat{N}^v_k, \tag{9}$$

$$-[\delta_{ir}\partial_3 + Y_{ip}(\partial_3 Y^{-1}_{pr})]\,\hat{\tau}'_{r3} = -sS_{ir}\hat{v}_r + s\,U_{ir}\,\hat{\tau}'_{r3} + \hat{N}^{\tau'}_i, \tag{10}$$

in which

$$T = \begin{pmatrix} 0 & 0 & -D_1 \\ 0 & 0 & -D_2 \\ -\frac{c_{13}}{c_{33}}D_1 & -\frac{c_{23}}{c_{33}}D_2 & 0 \end{pmatrix} \tag{11}$$

and

$$U = \begin{pmatrix} 0 & 0 & -\frac{c_5}{c_{55}}D_1\left(\frac{c_{13}}{c_3}\,.\right) \\ 0 & 0 & -\frac{c_4}{c_{44}}D_2\left(\frac{c_{23}}{c_3}\,.\right) \\ -\frac{c_3}{c_{33}}D_1\left(\frac{c_{55}}{c_5}\,.\right) & -\frac{c_3}{c_{33}}D_2\left(\frac{c_{44}}{c_4}\,.\right) & 0 \end{pmatrix}, \tag{12}$$

while

$$S = \begin{pmatrix} \frac{1}{c_5} & 0 & 0 \\ 0 & \frac{1}{c_4} & 0 \\ 0 & 0 & \frac{1}{c_3} \end{pmatrix} - \begin{pmatrix} \frac{c_5}{c_{55}}[D_1(d_{11}D_1\,.) + D_2(c_{66}D_2\,.)] & \frac{c_5}{c_{55}}[D_1(d_{12}D_2\,.) + D_2(c_{66}D_1\,.)] & 0 \\ \frac{c_4}{c_{44}}[D_2(d_{21}D_1\,.) + D_1(c_{66}D_2\,.)] & \frac{c_4}{c_{44}}[D_2(d_{22}D_2\,.) + D_1(c_{66}D_1\,.)] & 0 \\ 0 & 0 & 0 \end{pmatrix}, \tag{13}$$

where

$$d_{ij} = c_{ij} - \frac{c_{i3}c_{3j}}{c_{33}}, \quad i,j \in \{1,2\}. \tag{14}$$

Note that $d_{ij} = d_{ji}$. The notional source distributions follow as

$$\hat{N}^v = \begin{pmatrix} 2\hat{h}_{13} \\ 2\hat{h}_{23} \\ \frac{c_{13}}{c_{33}}\hat{h}_{11} + \frac{c_{23}}{c_{33}}\hat{h}_{22} + \hat{h}_{33} \end{pmatrix} \tag{15}$$

for the particle-velocity part, and

$$\hat{N}^{\tau'} = Y\left[\begin{pmatrix} \hat{f}_1 \\ \hat{f}_2 \\ \hat{f}_3 \end{pmatrix} - \begin{pmatrix} D_1[d_{11}\hat{h}_{11} + d_{12}\hat{h}_{22}] + D_2[2c_{66}\hat{h}_{12}] \\ D_2[d_{21}\hat{h}_{11} + d_{22}\hat{h}_{22}] + D_1[2c_{66}\hat{h}_{12}] \\ 0 \end{pmatrix}\right] \tag{16}$$

for the vertical-stress part.

2.4. *Wave field partitioning*

Using the up/down symmetry of the medium, we arrive at a convenient operator formalism by arranging the wave field quantities in the two field submatrices

$$\hat{\mathbf{F}}_1 = \begin{pmatrix} \hat{v}_1 \\ \hat{v}_2 \\ -\hat{\tau}'_{33} \end{pmatrix}, \qquad \hat{\mathbf{F}}_2 = \begin{pmatrix} -\hat{\tau}'_{13} \\ -\hat{\tau}'_{23} \\ \hat{v}_3 \end{pmatrix}. \tag{17}$$

The total field matrix is denoted by $\hat{\mathbf{F}}_I$. Here, uppercase Latin subscripts will range through the values 1, 2. In this notation, it is found that Eqs. (9) and (10) combine to

$$(\partial_3 \mathbf{I} + \Xi)_{I,J}\hat{\mathbf{F}}_J + s\hat{\mathbf{A}}_{I,J}\hat{\mathbf{F}}_J = \hat{\mathbf{N}}_I, \tag{18}$$

where

$$\Xi = \begin{pmatrix} 0 & \cdots & \cdots & \cdots & \cdots & 0 \\ \vdots & \cdots & \cdots & \cdots & \cdots & \vdots \\ \vdots & 0 & (Y(\partial_3 Y^{-1}))_{33} & 0 & 0 & \vdots \\ \vdots & 0 & 0 & (Y(\partial_3 Y^{-1}))_{11} & 0 & \vdots \\ \vdots & 0 & 0 & 0 & (Y(\partial_3 Y^{-1}))_{22} & \vdots \\ 0 & \cdots & \cdots & \cdots & \cdots & 0 \end{pmatrix} \tag{19}$$

is diagonal, and in which the elastodynamic system's matrix operator is partitioned into

$$\hat{\mathbf{A}} = \begin{pmatrix} 0 & \hat{\mathbf{A}}_{1,2} \\ \hat{\mathbf{A}}_{2,1} & 0 \end{pmatrix}, \tag{20}$$

with

$$\hat{\mathbf{A}}_{1,2} = \begin{pmatrix} C_{11} & 0 & T_{13} \\ 0 & C_{22} & T_{23} \\ U_{31} & U_{32} & S_{33} \end{pmatrix}, \qquad \hat{\mathbf{A}}_{2,1} = \begin{pmatrix} S_{11} & S_{12} & U_{13} \\ S_{21} & S_{22} & U_{23} \\ T_{31} & T_{32} & C_{33} \end{pmatrix}, \tag{21}$$

and has zero block matrices on the main diagonal. The form of Eq. (20) is maintained when going to monoclynic media, as long as the mirror plane of symmetry has its normal along the preferred (vertical) direction of propagation. The notional sources are correspondingly grouped together in

$$\hat{\mathbf{N}}_1 = \begin{pmatrix} \hat{N}_1^v \\ \hat{N}_2^v \\ \hat{N}_3^{\tau'} \end{pmatrix}, \qquad \hat{\mathbf{N}}_2 = \begin{pmatrix} \hat{N}_1^{\tau'} \\ \hat{N}_2^{\tau'} \\ \hat{N}_3^v \end{pmatrix}. \tag{22}$$

For alternative matrix representations and their symmetry properties the reader is referred to Ref. [24].

3. Decomposition into up- and downgoing waves

Via an appropriate linear transformation to be carried out on the field matrix, a wave-matrix formalism will be arrived at from which, at each depth level, a decomposition into up- and downgoing waves (with respect to the x_3-direction) will be manifest. The technique we develop here, is just a generalization of the diagonalization of a 2×2-matrix, with the extra complication that the elements of the matrix do not commute.

3.1. The characteristic equations

To achieve the decomposition we write

$$\hat{\mathbf{F}}_I = \hat{\mathbf{L}}_{I,J}\hat{\mathbf{W}}_J, \tag{23}$$

where $\hat{\mathbf{W}}_J$ is the wave matrix containing the up/down wave amplitudes. Via an appropriate choice of the composition operator $\hat{\mathbf{L}}_{I,J}$, Eq. (23) transforms Eq. (18) into

$$\hat{\mathbf{L}}_{I,J}\,(\partial_3\hat{\mathbf{W}}_J + s\hat{\Lambda}_{J,M}\hat{\mathbf{W}}_M) = -(\partial_3\hat{\mathbf{L}}_{I,J})\,\hat{\mathbf{W}}_J - \Xi_{I,J}\hat{\mathbf{L}}_{J,M}\,\hat{\mathbf{W}}_M + \hat{\mathbf{N}}_I, \tag{24}$$

as to make $\hat{\mathbf{A}}_{J,M}$, satisfying

$$\hat{\mathbf{A}}_{I,J}\hat{\mathbf{L}}_{J,M} = \hat{\mathbf{L}}_{I,J}\hat{\mathbf{A}}_{J,M}, \tag{25}$$

a block-diagonal matrix of operators. We arrange the 3×3-matrix elements of the composition matrix $\hat{\mathbf{L}}_{I,J}$ into columns (generalized eigenvectors) and write

$$\hat{\mathbf{L}}_I^{(+)} = \hat{\mathbf{L}}_{I,1}\,, \qquad \hat{\mathbf{L}}_I^{(-)} = \hat{\mathbf{L}}_{I,2}\,. \tag{26}$$

Let the diagonal matrix elements of $\hat{\mathbf{A}}_{J,M}$ be written as

$$\hat{\mathbf{A}}_{1,1} = \hat{\Gamma}^{(+)}, \qquad \hat{\mathbf{A}}_{2,2} = \hat{\Gamma}^{(-)}, \tag{27}$$

then Eq. (25) decomposes into the two systems of equations

$$\hat{\mathbf{A}}_{I,J}\hat{\mathbf{L}}_J^{(+)} = \hat{\mathbf{L}}_I^{(+)}\hat{\Gamma}^{(+)}, \tag{28}$$

$$\hat{\mathbf{A}}_{I,J}\hat{\mathbf{L}}_J^{(-)} = \hat{\mathbf{L}}_I^{(-)}\hat{\Gamma}^{(-)}. \tag{29}$$

Through mutual elimination, Eqs. (28) and (29) lead to decoupled equations for $\hat{\mathbf{L}}_1^{(\pm)}$ and $\hat{\mathbf{L}}_2^{(\pm)}$:

$$\hat{\mathbf{A}}_{1,2}\hat{\mathbf{A}}_{2,1}\hat{\mathbf{L}}_1^{(\pm)} = \hat{\mathbf{L}}_1^{(\pm)}\hat{\Gamma}^{(\pm)}\hat{\Gamma}^{(\pm)}, \tag{30}$$

$$\hat{\mathbf{A}}_{2,1}\hat{\mathbf{A}}_{1,2}\hat{\mathbf{L}}_2^{(\pm)} = \hat{\mathbf{L}}_2^{(\pm)}\hat{\Gamma}^{(\pm)}\hat{\Gamma}^{(\pm)}. \tag{31}$$

We call these equations the characteristic equations.

In our further analysis we need fractional and negative powers of the matrix operators $\hat{\mathbf{A}} = \hat{\mathbf{A}}_{2,1}\hat{\mathbf{A}}_{1,2}$ and $\hat{\mathbf{A}}_{1,2}$. Using Eq. (21), we obtain

$$\hat{\mathbf{A}} = \begin{pmatrix} \frac{1}{c_5^2} - \frac{c_5}{c_{55}}\left[D_1\left(d_{11}D_1\left(\frac{1}{c_5}\,.\right)\right) - D_1\left(\frac{c_{13}}{c_{33}}D_1\left(\frac{c_{55}}{c_5}\,.\right)\right) + D_2\left(c_{66}D_2\left(\frac{1}{c_5}\,.\right)\right)\right] \\ -\frac{c_4}{c_{44}}\left[D_2\left(d_{12}D_1\left(\frac{1}{c_5}\,.\right)\right) - D_2\left(\frac{c_{23}}{c_{33}}D_1\left(\frac{c_{55}}{c_5}\,.\right)\right) + D_1\left(c_{66}D_2\left(\frac{1}{c_5}\,.\right)\right)\right] \\ -\frac{1}{c_{33}}\left[D_1\left(\frac{c_{55}}{c_5}\,.\right) + c_{13}D_1\left(\frac{1}{c_5}\,.\right)\right] \end{pmatrix}$$

$$\begin{pmatrix} -\frac{c_5}{c_{55}}\left[D_1\left(d_{12}D_2\left(\frac{1}{c_5}\,.\right)\right) - D_1\left(\frac{c_{13}}{c_{33}}D_2\left(\frac{c_{44}}{c_4}\,.\right)\right) + D_2\left(c_{66}D_1\left(\frac{1}{c_5}\,.\right)\right)\right] \\ \frac{1}{c_4^2} - \frac{c_4}{c_{44}}\left[D_2\left(d_{22}D_2\left(\frac{1}{c_4}\,.\right)\right) - D_2\left(\frac{c_{23}}{c_{33}}D_2\left(\frac{c_{44}}{c_4}\,.\right)\right) + D_1\left(c_{66}D_1\left(\frac{1}{c_4}\,.\right)\right)\right] \\ -\frac{1}{c_{33}}\left[D_2\left(\frac{c_{44}}{c_4}\,.\right) + c_{23}D_2\left(\frac{1}{c_4}\,.\right)\right] \end{pmatrix} \tag{32}$$

$$\begin{pmatrix} -\frac{c_5}{c_{55}}\left[\frac{c_{55}}{c_5^2}D_1 + D_1\left(\frac{c_{13}}{c_3^2}\,.\right) - D_1\left(d_{11}D_1^2\,.\right) - 2D_2\left(c_{66}D_2D_1\,.\right) - D_1\left(d_{12}D_2^2\,.\right)\right] \\ -\frac{c_4}{c_{44}}\left[\frac{c_{44}}{c_4^2}D_2 + D_2\left(\frac{c_{23}}{c_3^2}\,.\right) - D_2\left(d_{12}D_1^2\,.\right) - 2D_1\left(c_{66}D_2D_1\,.\right) - D_2\left(d_{22}D_2^2\,.\right)\right] \\ \frac{1}{c_3^2} + \frac{c_{13}}{c_{33}}D_1^2 + \frac{c_{23}}{c_{33}}D_2^2 \end{pmatrix}.$$

To prove that this operator is elliptic, we let it act on the Fourier constituent $\exp(-i s\alpha_\mu x_\mu)$, where $i\alpha_\mu$ represent the horizontal components of the slowness vector, and thus obtain the symbol matrix $\hat{a} = \hat{a}(x_\mu, i\alpha_\nu, c_3^{-1}, c_4^{-1}, c_5^{-1}; x_3)$ of $\hat{\mathbf{A}}$ as

$$\hat{\mathrm{A}}\exp(-\mathrm{i}s\alpha_\mu x_\mu) = \hat{a}\exp(-\mathrm{i}s\alpha_\mu x_\mu). \tag{33}$$

Note that $i\alpha_\mu$ is the symbol of D_μ. The symbol matrix allows for a polyhomogeneous expansion of the type

$$\hat{a} = \hat{a}_2 + \hat{a}_1 + \hat{a}_0, \tag{34}$$

where $\hat{a}_2$, $\hat{a}_1$ and $\hat{a}_0$ are defined through

$$\hat{a}_{2-j}(x_\mu, s\mathrm{i}\alpha_\nu, sc_3^{-1}, sc_4^{-1}, sc_5^{-1}; x_3) = s^{2-j}\,\hat{a}_{2-j}(x_\mu, \mathrm{i}\alpha_\nu, c_3^{-1}, c_4^{-1}, c_5^{-1}; x_3), \quad j = 0, 1, 2. \tag{35}$$

Thus $\hat{a}_2$ is of the third, $\hat{a}_1$ is of the second, and $\hat{a}_0$ is of the zeroth degree in $\mathrm{i}\alpha_\nu$. The so-called principal symbol, $\hat{a}_2$, follows directly from Eq. (32) as

$$\hat{a}_2 = \begin{pmatrix} \dfrac{1}{c_5^2} + \left(\dfrac{d_{11}}{c_{55}} - \dfrac{c_{13}}{c_{33}}\right)\alpha_1^2 + \dfrac{c_{66}}{c_{55}}\alpha_2^2 & \dfrac{c_5}{c_4}\dfrac{1}{c_{55}}\left(d_{12} - c_{13}\dfrac{c_{44}}{c_{33}} + c_{66}\right)\alpha_1\alpha_2 & -ic_5\alpha_1\left[\left(1 + \dfrac{c_{13}}{c_{33}}\right)\dfrac{1}{c_5^2} + \dfrac{d_{11}}{c_{55}}\alpha_1^2 + \dfrac{2c_{66} + d_{12}}{c_{55}}\alpha_2^2\right] \\ \dfrac{c_4}{c_5}\dfrac{1}{c_{44}}\left(d_{12} - c_{23}\dfrac{c_{55}}{c_{33}} + c_{66}\right)\alpha_2\alpha_1 & \dfrac{1}{c_4^2} + \left(\dfrac{d_{22}}{c_{44}} - \dfrac{c_{23}}{c_{33}}\right)\alpha_2^2 + \dfrac{c_{66}}{c_{44}}\alpha_1^2 & -ic_4\alpha_2\left[\left(1 + \dfrac{c_{23}}{c_{33}}\right)\dfrac{1}{c_4^2} + \dfrac{2c_{66} + d_{12}}{c_{44}}\alpha_1^2 + \dfrac{d_{22}}{c_{44}}\alpha_2^2\right] \\ \left(\dfrac{c_{13} + c_{55}}{c_{33}}\right)\dfrac{(-\mathrm{i}\alpha_1)}{c_5} & \left(\dfrac{c_{23} + c_{44}}{c_{33}}\right)\dfrac{(-\mathrm{i}\alpha_2)}{c_4} & \dfrac{1}{c_3^2} - \dfrac{c_{13}}{c_{33}}\alpha_1^2 - \dfrac{c_{23}}{c_{33}}\alpha_2^2. \end{pmatrix} \tag{36}$$

At this point it is observed that the operator $\hat{\mathrm{A}}_2$ associated with $\hat{a}_2$ is the high-frequency approximation to $\hat{\mathrm{A}}$. To verify this, we use the property that in the high-frequency approximation the operator D_μ when acting on a wave constituent dominates D_μ when acting on a medium parameter. As a consequence, the eigenvalues of $\hat{a}_2$ must be the (local) vertical components of the slowness vectors squared. In particular, $c_3^{-1}, c_4^{-1}, c_5^{-1}$ are the slownesses of the different modes for vertical propagation ($\mathrm{i}\alpha_1 = \mathrm{i}\alpha_2 = 0$). Since

$$\det(\hat{a}_2) \neq 0 \quad \text{when } (\mathrm{i}\alpha_1, \mathrm{i}\alpha_2, c_3^{-1}, c_4^{-1}, c_5^{-1}) \neq (0,0,0,0,0), \tag{37}$$

the operator $\hat{\mathrm{A}}$ is elliptic with parameters $c_3^{-1}, c_4^{-1}, c_5^{-1}$. A similar analysis applies to the matrix $\hat{\mathbf{A}}_{1,2}$. These properties essentially guarantee that all powers of $\hat{\mathrm{A}}$ and $\hat{\mathbf{A}}_{1,2}$ exist. The symbol calculus over the extended phase space spanned by the coordinates $(x_\mu, \mathrm{i}\alpha_\nu, c_3^{-1}, c_4^{-1}, c_5^{-1})$ provides the tool to calculate these powers [4,25].

3.2. *The tensorial one-way wave equations*

To construct a non-trivial solution of Eqs. (30) and (31), we follow an Ansatz procedure. Assume that $\hat{\mathbf{L}}_2^{(\pm)}$ can be chosen such that

$$\hat{\mathbf{L}}_2^{(\pm)}\hat{\mathbf{A}}_{2,1}\hat{\mathbf{A}}_{1,2} = \hat{\mathbf{A}}_{2,1}\hat{\mathbf{A}}_{1,2}\hat{\mathbf{L}}_2^{(\pm)}, \tag{38}$$

i.e., assume that $\hat{\mathbf{L}}_2^{(\pm)}$ commutes with $\hat{\mathbf{A}}_{2,1}\hat{\mathbf{A}}_{1,2}$. Then, Eq. (31) can be rewritten as

$$\hat{\mathbf{L}}_2^{(\pm)}(\hat{\mathbf{A}}_{2,1}\hat{\mathbf{A}}_{1,2} - \hat{\Gamma}^{(\pm)}\hat{\Gamma}^{(\pm)}) = 0. \tag{39}$$

Using the condition that $\mathrm{Ker}(\hat{\mathbf{L}}_2^{(\pm)}) = 0$, we find that the $\hat{\Gamma}^{(\pm)}$ must satisfy the equation

$$\hat{\mathbf{A}}_{2,1}\hat{\mathbf{A}}_{1,2} - \hat{\Gamma}^{(\pm)}\hat{\Gamma}^{(\pm)} = 0. \tag{40}$$

From this equation it follows that

$$\hat{\Gamma}^{(\pm)} = \pm\hat{\Gamma} \quad \text{with} \quad \hat{\Gamma} = (\hat{\mathbf{A}}_{2,1}\hat{\mathbf{A}}_{1,2})^{1/2} = \hat{\mathbf{A}}, \tag{41}$$

for a properly defined square root of the (positive definite) matrix operator $\hat{\mathbf{A}}_{2,1}\hat{\mathbf{A}}_{1,2}$. Using Eq. (40) in Eq. (30), one obtains

$$\hat{\mathbf{A}}_{1,2}\hat{\mathbf{A}}_{2,1}\hat{\mathbf{L}}_1^{(\pm)} = \hat{\mathbf{L}}_1^{(\pm)}\hat{\mathbf{A}}_{2,1}\hat{\mathbf{A}}_{1,2}, \tag{42}$$

of which obviously $\hat{\mathbf{L}}_1^{(\pm)} = \hat{\mathbf{A}}_{1,2}$ is a solution. Using this in Eqs. (28)–(29), it follows that a possible solution is given by

$$\hat{\mathbf{L}}_2^{(\pm)} = \pm\hat{\Gamma}, \qquad \hat{\mathbf{L}}_1^{(\pm)} = \hat{\mathbf{A}}_{1,2}. \tag{43}$$

Since $\hat{\mathbf{L}}_2^{(\pm)}$ as given by Eq. (43) satisfies Eq. (38), our starting assumption is justified. Thus, the composition matrix $\hat{\mathbf{L}}$ becomes (cf. Eq. (26))

$$\hat{\mathbf{L}} = \begin{pmatrix} \hat{\mathbf{A}}_{1,2} & \hat{\mathbf{A}}_{1,2} \\ \hat{\Gamma} & -\hat{\Gamma} \end{pmatrix}. \tag{44}$$

From this the corresponding decomposition matrix $\hat{\mathbf{L}}^{-1}$ is found as

$$\hat{\mathbf{L}}^{-1} = \frac{1}{2}\begin{pmatrix} \hat{\mathbf{A}}_{1,2}^{-1} & \hat{\Gamma}^{-1} \\ \hat{\mathbf{A}}_{1,2}^{-1} & -\hat{\Gamma}^{-1} \end{pmatrix}, \tag{45}$$

for a properly defined inverse of the matrix $\hat{\mathbf{A}}_{1,2}$.

Upon applying $\hat{\mathbf{L}}^{-1}$ to Eq. (24), it is found that

$$\partial_3\hat{\mathbf{W}}_I + s\hat{\mathbf{A}}_{I,M}\hat{\mathbf{W}}_M = -(\hat{\mathbf{L}}^{-1})_{I,M}(\partial_3\hat{\mathbf{L}}_{M,K})\hat{\mathbf{W}}_K - (\hat{\mathbf{L}}^{-1})_{I,M}\Xi_{M,J}\hat{\mathbf{L}}_{J,K}\hat{\mathbf{W}}_K + (\hat{\mathbf{L}}^{-1})_{I,M}\hat{\mathbf{N}}_M. \tag{46}$$

Since the matrix $\hat{\mathbf{A}}_{I,M}$ in the left-hand side is block diagonal (cf. Eq. (27)), Eq. (46) represents the desired coupled system of tensorial one-way wave equations, in which $\hat{\mathbf{W}}_1$ is representative for the downgoing waves and $\hat{\mathbf{W}}_2$ for the upgoing waves. As far as the left-hand side in Eq. (46) is concerned, these waves travel independently and $\hat{\Gamma}$ is their *vertical slowness* matrix. In the right-hand side of Eq. (46), the up- and downgoing wave constituents are coupled at any depth level where $\partial_3\hat{\mathbf{L}}_{M,K}$ or $\partial_3 Y$ differ from zero.

The procedure followed thus far has achieved a decomposition of the total wave motion into collections of downgoing and upgoing constituents, while a separation into the different polarization states has not yet taken place. This separation will be discussed in the next section.

4. Decomposition into polarization states

For the decomposition into polarization states the block-diagonal matrix $\hat{\mathbf{A}}_{I,M}$ has to be completely diagonalized. The high-frequency approximation to this procedure has the convenient property that each of the elements of the matrix operators involved commutes with one another. In this approximation the principal symbol $\hat{a}_2$ replaces $\hat{a}$, which leads to a corresponding approximation $\hat{\mathbf{A}}_2$ of $\hat{\mathbf{A}}$ via Eq. (33). In the present section we explicitly determine the vertical slowness matrix, the coupled one-way wave equations for the polarization states, and the composition matrix, on the level of the principal symbols only. Beyond the high frequency approximation one has to use the full vertical slowness operator to account for lateral heterogeneity.

To achieve this we write as a first step each wave quantity as its spatial horizontal Fourier representation. Then the relevant operators can be expressed in terms of their symbols. For $\hat{\mathbf{F}}_2$ this implies

$$\hat{\mathbf{F}}_2(x_\mu) = (s/2\pi)^2 \int_{\alpha_\nu \in \mathcal{R}^2} \tilde{\mathbf{F}}_2(\mathrm{i}\alpha_\nu) \exp(\mathrm{i}s\alpha_\sigma x_\sigma)\, \mathrm{d}\alpha_1\, \mathrm{d}\alpha_2, \tag{47}$$

and hence

$$(\hat{\mathbf{A}}(x_\kappa, D_\lambda)\, \hat{\mathbf{F}}_2)(x_\mu) = \int_{x'_\nu \in \mathcal{R}^2} \hat{\mathcal{A}}(x_\mu, x'_\nu)\, \hat{\mathbf{F}}_2(x'_\nu)\, \mathrm{d}x'_1\, \mathrm{d}x'_2, \tag{48}$$

in which, with the use of Eq. (33),

$$\hat{\mathcal{A}}(x_\mu, x'_\nu) = (s/2\pi)^2 \int_{\alpha_\nu \in \mathcal{R}^2} \hat{a}(x_\mu, \mathrm{i}\alpha_\nu) \exp[\mathrm{i}s\alpha_\sigma(x'_\sigma - x_\sigma)]\, \mathrm{d}\alpha_1\, \mathrm{d}\alpha_2. \tag{49}$$

The kernel $\hat{\mathcal{A}}$ allows for a matrix representation upon discretizing the wave field. Similar relations hold for the other relevant operators in our formalism. To indicate the symbols in our calculus on the level of their principal parts, we use the symbol $\tilde{}$. In this notation we have

$$\tilde{\mathbf{A}}_{2,1}\tilde{\mathbf{A}}_{1,2} = \tilde{\mathbf{A}} = \tilde{\mathbf{A}}_2 = \hat{a}_2. \tag{50}$$

4.1. The vertical slowness matrix

The principal part $\tilde{\Gamma}$ of the vertical slowness matrix, as this follows from Eq. (41), will now be determined with the aid of an eigenvalue approach. Let the eigenvalues of $\tilde{\mathbf{A}}_{2,1}\tilde{\mathbf{A}}_{1,2}$ constitute the 3×3 diagonal matrix $\tilde{\Pi}$ and let $\tilde{M}$ be the corresponding matrix of eigenvectors. Then

$$\tilde{\mathbf{A}}_{2,1}\tilde{\mathbf{A}}_{1,2}\tilde{M} = \tilde{M}\tilde{\Pi}. \tag{51}$$

Employing the determinantal equation associated with Eq. (51), it is found that for our medium with orthorhombic symmetry

$$\tilde{\Pi} = \begin{pmatrix} \gamma_1^2 & 0 & 0 \\ 0 & \gamma_2^2 & 0 \\ 0 & 0 & \gamma_3^2 \end{pmatrix}, \tag{52}$$

in which $\gamma_1^2, \gamma_2^2, \gamma_3^2$, in general, follow from Cardano's formula for the cubic equation. Upon rewriting Eq. (51) as $\tilde{\mathbf{A}}_{2,1}\tilde{\mathbf{A}}_{1,2} = \tilde{M}\tilde{\Pi}\tilde{M}^{-1}$ and comparing this result with Eq. (40), the vertical slowness matrix follows as

$$\tilde{\Gamma} = \tilde{M}\tilde{\Pi}^{1/2}\tilde{M}^{-1}, \tag{53}$$

where the diagonal elements of $\tilde{\Pi}^{1/2}$ are $\gamma_1, \gamma_2, \gamma_3$ with $\mathrm{Re}\{\gamma_{1,2,3}\}(\mathrm{i}\alpha_1, \mathrm{i}\alpha_2) \geq 0$. In particular, $\gamma_1(0,0) = c_5^{-1}, \gamma_2(0,0) = c_4^{-1}, \gamma_3(0,0) = c_3^{-1}$. For any power z of $\tilde{\Gamma}$ we then have

$$\tilde{\Gamma}^z = \sum_{j=1}^{3} \tilde{\Gamma}^{(j)} \gamma_j^z, \tag{54}$$

where (no sum over j)

$$\tilde{\Gamma}^{(j)}_{k\ell} = \tilde{M}_{kj}(\tilde{M}^{-1})_{j\ell}. \tag{55}$$

Since $\tilde{M} = \tilde{M}(\gamma_j^2)$ and $\tilde{M}^{-1} = \tilde{M}^{-1}(\gamma_j^2)$, also $\tilde{\Gamma}^{(i)} = \tilde{\Gamma}^{(i)}(\gamma_j^2)$.

The determination of $\tilde{\mathbf{A}}_{1,2}^{-1}$ is standard. Now that the expressions for $\tilde{\Gamma}$, $\tilde{\Gamma}^{-1}$ and $\tilde{\mathbf{A}}_{1,2}^{-1}$ have been derived, the up/down composition matrix $\tilde{\mathbf{L}}$ as given by Eq. (44) and the up/down decomposition matrix $\tilde{\mathbf{L}}^{-1}$ as given by Eq. (45) are known.

4.2. The scalar one-way wave equations

To arrive at the further decomposition of the up- and downgoing wave constituents into their polarization states, the matrix $\tilde{\Gamma}$ as it occurs in Eq. (46) in the elements of $\tilde{\mathbf{A}}$ (cf. Eq. (27)) must be diagonalized. Let $\tilde{\mathbf{V}}_J$ be the matrix of amplitudes of the polarization states, i.e.,

$$\tilde{\mathbf{W}}_J = \tilde{M}\tilde{\mathbf{V}}_J. \tag{56}$$

Using $\tilde{\Gamma}\tilde{M}\tilde{\mathbf{V}}_J = \tilde{M}\tilde{\Pi}^{1/2}\tilde{\mathbf{V}}_J$ in Eq. (46), premultiplying the result by $\tilde{M}^{-1}$ and using Eq. (54), we get

$$\begin{aligned}\partial_3\tilde{\mathbf{V}}_I + s\,\epsilon_{I,M}\tilde{\Pi}^{1/2}\tilde{\mathbf{V}}_M = -[\tilde{M}^{-1}(\partial_3\tilde{M})\delta_{I,K} + \tilde{M}^{-1}\{(\tilde{\mathbf{L}}^{-1})_{I,M}(\partial_3\tilde{\mathbf{L}}_{M,K})\\ + (\hat{\mathbf{L}}^{-1})_{I,M}\Xi_{M,J}\hat{\mathbf{L}}_{J,K}\}\tilde{M}]\tilde{\mathbf{V}}_K + \tilde{M}^{-1}(\tilde{\mathbf{L}}^{-1})_{I,M}\tilde{\mathbf{N}}_M,\end{aligned} \tag{57}$$

where

$$\epsilon = \begin{pmatrix} 1 & 0 \\ 0 & -1 \end{pmatrix}. \tag{58}$$

Observe that the first term on the right-hand side of Eq. (57) does contain a down/down and up/up interaction term that is responsible for the coupling between polarization states, while the second term is representative for the up/down interaction. In anisotropic media, the coupling between the polarization states may be large even in the high-frequency approximation, viz., in directions associated with singularities of the (local) slowness surface.

4.3. The normalization of the composition matrix

To arrive at the 6×6 composition matrix of the polarization states, we set

$$\tilde{\mathbf{M}} = \begin{pmatrix} \tilde{M} & 0 \\ 0 & \tilde{M} \end{pmatrix}. \tag{59}$$

On account of Eqs. (23), (44), (53) and (56), the composition matrix that constructs the field matrix out of the matrix of polarization states follows as the tensor product

$$\tilde{\mathbf{L}}\tilde{\mathbf{M}} = \begin{pmatrix} \tilde{\mathbf{X}} & \tilde{\mathbf{X}} \\ \tilde{\mathbf{Y}} & -\tilde{\mathbf{Y}} \end{pmatrix}, \tag{60}$$

in which

$$\tilde{\mathbf{X}} = \tilde{\mathbf{A}}_{1,2}\tilde{M}, \qquad \tilde{\mathbf{Y}} = \tilde{M}\tilde{\Pi}^{1/2}. \tag{61}$$

The matrix $\tilde{\mathbf{L}}\tilde{\mathbf{M}}$ diagonalizes the elastodynamic system's matrix $\tilde{\mathbf{A}}$ (cf. Eqs. (25), (27) and (53)) according to

$$\tilde{\mathbf{A}}\tilde{\mathbf{L}}\tilde{\mathbf{M}} = \tilde{\mathbf{L}}\tilde{\mathbf{M}}\begin{pmatrix} \tilde{\Pi}^{1/2} & 0 \\ 0 & -\tilde{\Pi}^{1/2} \end{pmatrix}. \tag{62}$$

So far, the normalization of the eigenvectors of the polarization states that constitute $\tilde{\mathbf{M}}$ is arbitrary. Since the elastodynamic system's matrix $\tilde{\mathbf{A}}$ satisfies the symplectic property

$$\tilde{\mathbf{A}}^{\mathrm{T}} J_{\dot{Y}} = J_Y \tilde{\mathbf{A}}, \tag{63}$$

i.e.,

$$\tilde{\mathbf{A}}_{2,1}^{\mathrm{T}} = Y^{-1}\tilde{\mathbf{A}}_{2,1}Y \quad \text{and} \quad \tilde{\mathbf{A}}_{1,2}^{\mathrm{T}} = Y^{-1}\tilde{\mathbf{A}}_{1,2}Y, \tag{64}$$

in which

$$J_Y = \begin{pmatrix} 0 & Y^{-1} \\ Y^{-1} & 0 \end{pmatrix} \tag{65}$$

is the scaled symplectic matrix, the existence of eigenvectors that satisfy the vertical power flux orthogonality and normalization condition,

$$(\tilde{\mathbf{L}}\tilde{\mathbf{M}})^{\mathrm{T}} J_Y (\tilde{\mathbf{L}}\tilde{\mathbf{M}}) = \mathbf{K} \quad \text{with} \quad \mathbf{K} = \begin{pmatrix} I & 0 \\ 0 & -I \end{pmatrix}, \tag{66}$$

is guaranteed. In this normalization, using Eqs. (60) and (65), it follows that

$$2\tilde{\mathbf{X}}^{\mathrm{T}} Y^{-1} \tilde{\mathbf{Y}} = I. \tag{67}$$

Starting from a particular normalization, different ones can be chosen at one's convenience upon replacing the given $\tilde{M}$ by $\tilde{M}\beta$, where β is a 3×3 diagonal matrix. Then $\tilde{\mathbf{X}}^{\mathrm{T}}$ is replaced by $\beta\tilde{\mathbf{X}}^{\mathrm{T}}$, $\tilde{\mathbf{Y}}$ by $\tilde{\mathbf{Y}}\beta$, and the right-hand side of Eq. (67) by $\beta^2 I$.

As indicated by Schoenberg and Protazio [26], the structure of Eq. (60) also simplifies the structure of the Zoeppritz equation for the reflection and transmission at an interface.

4.4. *Two special cases*

Two special cases will be discussed: the hexagonal (TIV) and the isotropic medium. For these two cases the expressions for $\tilde{\Pi}$ and $\tilde{M}$, which serve as a starting point for the parabolic approximations to be discussed in Section 5, are relatively simple, although (complicated) analytic expressions for these matrices exist for the general orthorhombic case.

For the *hexagonal* (TIV) medium, we have $c_{11} = c_{22}$, $c_{13} = c_{23}$, $c_{44} = c_{55}$, $c_{66} = (c_{11} - c_{12})/2$. Then Eqs. (51) and (52) lead to

$$\gamma_1^2 = \frac{\rho}{c_{55}} + \frac{c_{66}}{c_{55}}\alpha_\mu\alpha_\mu \qquad \text{(qSH)} \tag{68}$$

$$\gamma_2^2 = \frac{1}{2c_{33}c_{55}}\left\{b + [b^2 - 4c_{33}c_{55}(c_{11}\alpha_\mu\alpha_\mu + \rho)(c_{55}\alpha_\nu\alpha_\nu + \rho)]^{1/2}\right\} \qquad \text{(qSV)} \tag{69}$$

$$\gamma_3^2 = 7\frac{1}{2c_{33}c_{55}}\left\{b - [b^2 - 4c_{33}c_{55}(c_{11}\alpha_\mu\alpha_\mu + \rho)(c_{55}\alpha_\nu\alpha_\nu + \rho)]^{1/2}\right\} \qquad \text{(qP)} \tag{70}$$

where

$$b = (c_{33} + c_{55})\rho + [c_{11}c_{33} - (c_{13} + c_{55})^2 + c_{55}^2]\alpha_\mu\alpha_\mu. \tag{71}$$

We select a mixed normalization, in which the matrix $\tilde{M}$ of eigenvectors gets the form

$$\tilde{M} = \begin{pmatrix} -\dfrac{\mathrm{i}\alpha_2}{(\alpha_\mu\alpha_\mu)^{1/2}} & -\sqrt{\dfrac{c_{55}}{\rho}}\,2\mathrm{i}\alpha_1(\alpha_\mu\alpha_\mu)^{1/2}\left\{\dfrac{(c_{13}+c_{33})\rho + (c_{11}c_{33} - c_{13}^2)\alpha_\mu\alpha_\mu}{2c_{33}c_{55}\gamma_3^2 - 2\rho c_{55} + 2c_{13}c_{55}\alpha_\nu\alpha_\nu}\right\} \\ \dfrac{\mathrm{i}\alpha_1}{(\alpha_\mu\alpha_\mu)^{1/2}} & -\sqrt{\dfrac{c_{55}}{\rho}}\,2\mathrm{i}\alpha_2(\alpha_\mu\alpha_\mu)^{1/2}\left\{\dfrac{(c_{13}+c_{33})\rho + (c_{11}c_{33} - c_{13}^2)\alpha_\mu\alpha_\mu}{2c_{33}c_{55}\gamma_3^2 - 2\rho c_{55} + 2c_{13}c_{55}\alpha_\nu\alpha_\nu}\right\} \\ 0 & -(\alpha_\mu\alpha_\mu)^{1/2} \end{pmatrix}$$

$$\begin{pmatrix} \sqrt{\frac{c_{55}}{\rho}}\, 2\mathrm{i}\alpha_1 \left\{ \frac{(c_{13}+c_{33})\rho + (c_{11}c_{33}-c_{13}^2)\,\alpha_\mu\alpha_\mu}{2c_{33}c_{55}\gamma_2^2 - 2\rho c_{55} + 2c_{13}c_{55}\,\alpha_\nu\alpha_\nu} \right\} \\ \sqrt{\frac{c_{55}}{\rho}}\, 2\mathrm{i}\alpha_2 \left\{ \frac{(c_{13}+c_{33})\rho + (c_{11}c_{33}-c_{13}^2)\,\alpha_\mu\alpha_\mu}{2c_{33}c_{55}\gamma_2^2 - 2\rho c_{55} + 2c_{13}c_{55}\,\alpha_\nu\alpha_\nu} \right\} \\ 1 \end{pmatrix}. \tag{72}$$

For the *isotropic* medium, we have $c_{11} = c_{22} = c_{33} = \lambda + 2\mu$, $c_{12} = c_{13} = c_{23} = \lambda$, $c_{44} = c_{55} = c_{66} = \mu$, where λ, μ are the Lamé parameters. The simplifications amount to (cf. Eq. (14))

$$d_{11} = d_{22} = \frac{4\mu(\lambda+\mu)}{\lambda+2\mu}, \qquad d_{12} = \frac{2\lambda\mu}{\lambda+2\mu}, \tag{73}$$

while $c_3 = c_P = [(\lambda+2\mu)/\rho]^{1/2}$ is the compressional and $c_4 = c_5 = c_S = [\mu/\rho]^{1/2}$ are the shear wave speeds. In view of our analysis in Section 6, it is convenient to express λ in terms of μ and ζ in accordance with

$$\zeta = \frac{\lambda+\mu}{\lambda+2\mu} \tag{74}$$

with $1/4 < \zeta < 1$. Then $c_P^{-2} = (1-\zeta)c_S^{-2}$. Thus

$$\gamma_1^2 = \gamma_2^2 = \gamma_S^2 = \frac{\rho}{\mu} + \alpha_\nu\alpha_\nu \qquad \text{(SH,SV)} \tag{75}$$

$$\gamma_3^2 = \gamma_P^2 = \frac{\rho}{\mu}(1-\zeta) + \alpha_\nu\alpha_\nu \qquad \text{(P)}. \tag{76}$$

To simplify the notation further, we employ the auxiliary quantity

$$\chi = \frac{\rho}{2\mu} + \alpha_\nu\alpha_\nu. \tag{77}$$

Then

$$\tilde{M} = \begin{pmatrix} -\frac{\mathrm{i}\alpha_2}{(\alpha_\mu\alpha_\mu)^{1/2}} & -\frac{\mathrm{i}\alpha_1}{(\alpha_\mu\alpha_\mu)^{1/2}}\sqrt{\frac{\mu}{\rho}}2\chi & 2\mathrm{i}\alpha_1\sqrt{\frac{\mu}{\rho}} \\ \frac{\mathrm{i}\alpha_1}{(\alpha_\mu\alpha_\mu)^{1/2}} & -\frac{\mathrm{i}\alpha_2}{(\alpha_\mu\alpha_\mu)^{1/2}}\sqrt{\frac{\mu}{\rho}}2\chi & 2\mathrm{i}\alpha_2\sqrt{\frac{\mu}{\rho}} \\ 0 & -(\alpha_\mu\alpha_\mu)^{1/2} & 1 \end{pmatrix}. \tag{78}$$

These examples will be used in the next section to illustrate the parabolic approximations.

5. The parabolic approximation

In this section the general features of the parabolic approximation when carried out on the vertical slowness operator (as given by Eq. (53)) will be discussed on the level of the principal symbol of the latter. The purpose of the parabolic approximation is to arrive at a spatial finite-difference representation of the vertical slowness operator $\hat{\Gamma}$ (which is, in fact, a sparse matrix representation of its kernel, cf. Ref. [4]). The latter procedure implies similar representations for $\hat{\Lambda}$, $\hat{\mathbf{L}}$ and $\hat{\mathbf{L}}^{-1}$ (cf. Eq. (46)). To achieve this purpose, the vertical slowness symbol must be approximated by a matrix with either polynomial or rational elements: its elements will be expanded as functions of the horizontal slownesses. It is conjectured that the expansion of the principal symbol implies uniquely an expansion of the higher-order symbols.

The approximations involve either a polynomial (Taylor) expansion about a particular direction, or a rational (Thiele) expansion about a particular direction (see Ref. [6]), or either a polynomial (Lagrange)

interpolation or a rational (Newton) interpolation [27] with judiciously chosen directional abscissas. Both the Taylor and the Thiele approximations can be straightforwardly carried out on the conditions of mild anisotropy [28]:
- $\min\{c_{11}, c_{22}, c_{33}\} > \max\{c_{44}, c_{55}, c_{66}\}$; i.e., the slowest bulk wave along any coordinate axis is faster than the fastest shear wave along any coordinate axis;
- $c_{23} + c_{44} > 0$, $c_{13} + c_{55} > 0$, $c_{12} + c_{66} > 0$; i.e., the longitudinally polarized wave is always faster than the transverselly polarized wave in any of the coordinate planes;
- there is no triplication of the slower one of the two waves that have their polarizations in any of the symmetry planes as their plane of propagation (this condition can be worked out along the lines indicated by Payton [29].

These conditions imply that all points on the cross sections of the real slowness surface with the symmetry planes are convex elliptic about the vertical axis. The third condition of mild anisotropy can be relaxed to: no triplication on an axis of symmetry or in a plane perpendicular to it. If we want to approximate an off-axis triplication (as it, for example, may occur in the qSV wave in a hexagonal medium), the interpolation schemes are the only choice. As far as their respective finite-difference representations (through the vertical slowness operator matrix) are concerned, the polynomial approximations allow for explicit schemes whereas the rational approximations necessarily lead to implicit schemes (see also Ref. [3]).

5.1. Constraints

To obtain a physically acceptable approximation at all, i.e., one that preserves the characteristics of the propagating waves, the following constraints are imposed:
- the ellipticity of $\hat{\mathbf{A}}$ is preserved;
- the singularities on the wave front near the preferred direction of propagation are preserved;
- artificial multiple points of the sheets of the approximate real slowness surface are avoided;
- artificial precursors to the *exact* wave front are avoided;
- the Green's functions of the approximated tensorial one-way wave equations have a physically acceptable space-time counterpart.

5.2. The two-level parabolic approximation scheme

Our two-level parabolic approximation scheme is characterized by an independent treatment of the roots γ_j, $j = 1, 2, 3$ and their squares γ_j^2 as they occur in Eq. (54). For their parabolic approximations we use the notation $\gamma_j^{(p)}$ and $(\gamma_j^2)^{(p)}$, respectively. Through this procedure the accuracy is best maintained, although one might argue that it shall suffer from some inconsistency. The minimal order of the approximation is determined by the canonical form of the slowness surface parametrization following from singularity theory.

In the correspondingly approximated first-order hyperbolic system, we first retain the relation (cf. Eqs. (41) and (54))

$$\tilde{\mathbf{A}}_{2,1}\tilde{\mathbf{A}}_{1,2} = \sum_{j=1}^{3} \tilde{\Gamma}^{(j)}((\gamma_j^2)^{(p)})\,(\gamma_j^{(p)})^2. \tag{79}$$

Secondly, we choose to keep the matrix $\tilde{\mathbf{A}}_{1,2}$ in its exact form, since it is already polynomial in the horizontal slownesses. As a consequence, we must replace the matrix $\tilde{\mathbf{A}}_{2,1}$ by its parabolic counterpart

$$\tilde{\mathbf{A}}_{2,1} = \sum_{j=1}^{3} \tilde{\Gamma}^{(j)}((\gamma_j^2)^{(p)})\,\tilde{\mathbf{A}}_{1,2}^{-1}\,(\gamma_j^{(p)})^2. \tag{80}$$

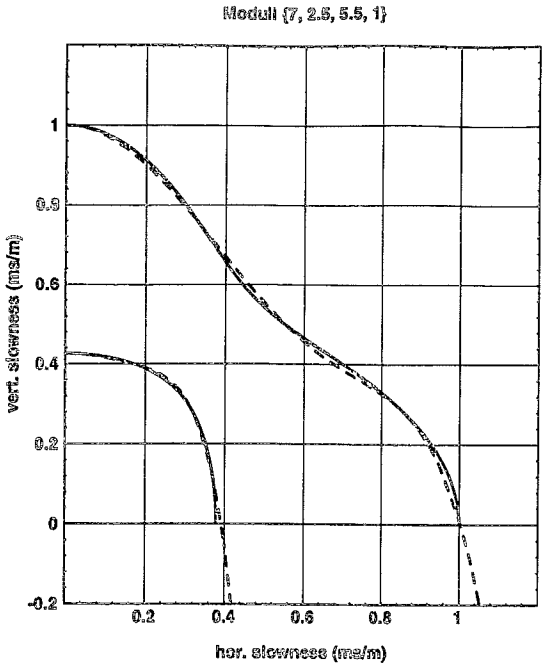

Fig. 1. The exact (solid line) and approximate (dashed line) qP and qSV sheets of the slowness surface of a particular TIV medium (4-point polynomial interpolation in the horizontal slownesses squared).

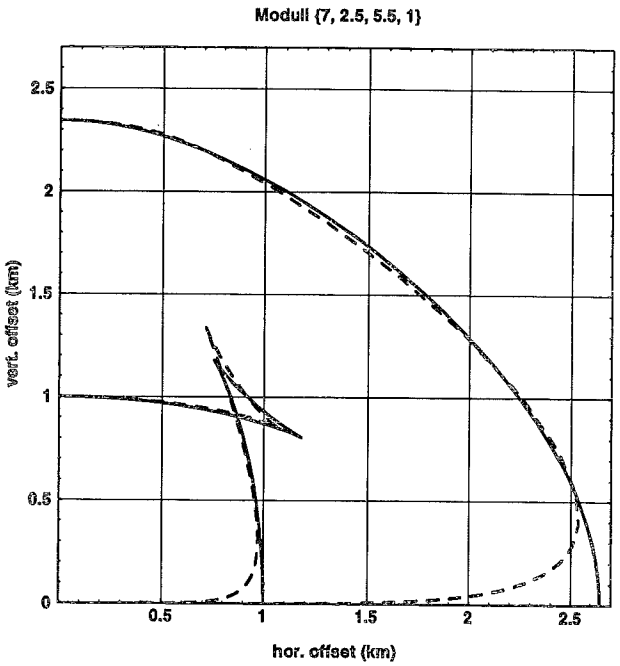

Fig. 2. The exact (solid line) and approximate (dashed line) qP and qSV sheets of the group velocity surface associated with the slowness surface of Fig. 1.

For an isotropic or elliptically anisotropic medium γ_j^2 need not be approximated at all, whereas for general TIV media sensible expansions about the elliptically anisotropic case exist. In those cases where also γ_j^2 is subject to an expansion, the orders to which γ_j and γ_j^2 are expanded must be mutually compatible, i.e., should be equal.

Illustrations of the different order Taylor and Thiele expansions for isotropic media have been given in Ref. [6]. In particular, the first-order approximations γ_P^I and γ_S^I of γ_P and γ_S are given by

$$\gamma_{P,S}^I = c_{P,S}^{-1} + (1/2)\, c_{P,S}\alpha_\mu\alpha_\mu. \tag{81}$$

For a hexagonal (TIV) medium with $c_{11}/\rho = 7, c_{13}/\rho = 2.5, c_{33}/\rho = 5.5, c_{55}/\rho = 1$, $(c_{66}/\rho = 1.463)$ Fig. 1 shows the result of a 4-point Lagrange interpolation in the square horizontal slowness applied to γ_2 (qSV) and γ_3 (qP) based on matching the vertical slownesses at equally spaced phase angles up to 72 degrees (which gives an optimal fit) away from vertical. Fig. 2 shows the corresponding group velocity surfaces that follow by taking the polar reciprocal of the real slowness surface: introduce the function

$$H(s_1, s_2, s_3) = \prod_{j=1}^{3} [s_3 - \gamma_j^{(p)}(is_1, is_2)]. \tag{82}$$

The approximated (phase) slowness surface is then given by

$$H = 0, \tag{83}$$

and the corresponding group velocity surface follows as

$$\left. \frac{\partial_{s_i} H}{s_k\, \partial_{s_k} H} \right|_{H=0}. \tag{84}$$

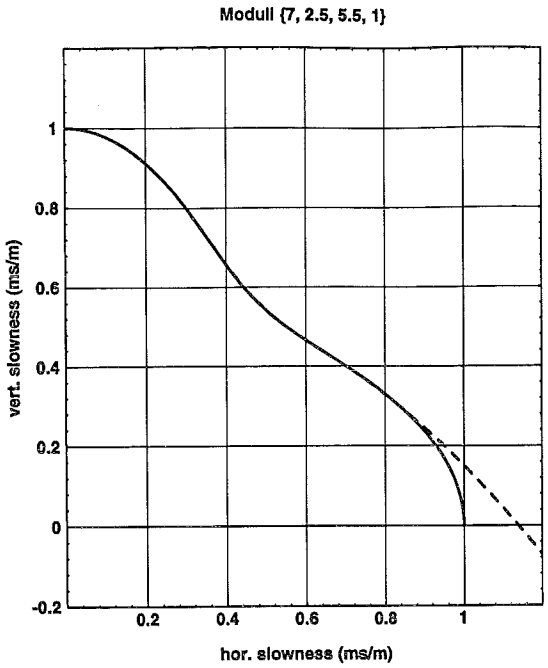

Fig. 3. The exact (solid line) and approximate (dashed line) qSV sheet of the slowness surface of a particular TIV medium (8-point rational interpolation in the horizontal slownesses squared).

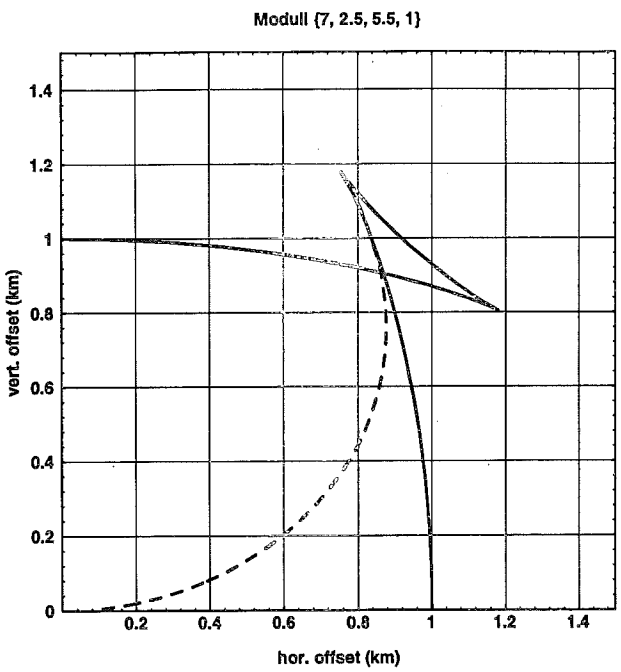

Fig. 4. The exact (solid line) and approximate (dashed line) qSV sheet of the group velocity surface associated with the slowness surface of Fig. 3.

Fig. 3 shows an 8-point Newton interpolation in the square horizontal slowness of γ_2 based on matching the qSV vertical slowness at equally spaced phase angles up to 70 degrees. Fig. 4 shows the corresponding group velocity surface. The latter results fit in with Kitchenside's 9-point like approximation; however, we employ odd order rather than his even order interpolation schemes. The explicit expressions are given in Appendix A. The approximations in Figs. 1 and 3 lead to the most compatible matrix equations in their respective implicit finite difference representations for down/upward continuation.

Note that in the rational approximations complex poles in the horizontal slowness (α_1-) plane turn up. Their contribution yields time-domain counterparts that occur in the wake of the wave phenomena and do not disturb the accuracy of the results right at or just behind the wave fronts.

The approximations to γ_1 and γ_1^2 (qSH) are standard and are not shown.

5.3. *The 'moving frame' of reference*

For the numerical implementation of Eq. (46), it is advantageous to transform the constituents of this equation to their respective 'moving' frames of reference. Using that in the limit $\alpha_{1,2} \to 0$ the matrix $\hat{\Gamma}$ becomes diagonal, it is found that the change to the moving frames is given by $\hat{\mathbf{W}}_{1,2} \to \hat{\mathbf{w}}_{1,2}$ with

$$\hat{\mathbf{W}}_1 = \exp(-s\mathbf{T})\,\hat{\mathbf{w}}_1, \quad \hat{\mathbf{W}}_2 = \exp(s\mathbf{T})\,\hat{\mathbf{w}}_2 \tag{85}$$

with the vertical travel time matrix defined as

$$\mathbf{T} = \int_{\zeta=0}^{x_3} C\,\mathrm{d}\zeta, \tag{86}$$

in which C is given by Eq. (6). For near vertical propagation in a source-free domain our parabolic approximation scheme is closely related to the 'moving frame' of reference approach as it has been discussed by Claerbout [2] for the propagation in a fluid medium. To show this we restart from Eqs. (18) and (20), and substitute in them the expressions

$$\hat{\mathbf{F}}_{1,2} = \exp(-s\mathbf{T})\,\hat{\mathbf{f}}_{1,2}. \tag{87}$$

The procedure leads to (use that C is diagonal)

$$\partial_3\hat{\mathbf{f}}_1 - sC\hat{\mathbf{f}}_1 + s\hat{\mathbf{A}}'_{1,2}\hat{\mathbf{f}}_2 = 0, \tag{88}$$

$$\partial_3\hat{\mathbf{f}}_2 - (sC - \Xi'_{2,2})\,\hat{\mathbf{f}}_2 + s\hat{\mathbf{A}}'_{2,1}\hat{\mathbf{f}}_1 = 0, \tag{89}$$

where

$$\hat{\mathbf{A}}'_{1,2} = \exp(s\mathbf{T})\hat{\mathbf{A}}_{1,2}\exp(-s\mathbf{T}), \quad \hat{\mathbf{A}}'_{2,1} = \exp(s\mathbf{T})\hat{\mathbf{A}}_{2,1}\exp(-s\mathbf{T}) \tag{90}$$

and

$$\Xi'_{2,2} = \exp(s\mathbf{T})\,\Xi_{2,2}\exp(-s\mathbf{T}). \tag{91}$$

Eliminating $\hat{\mathbf{f}}_2$ from the equations above and neglecting the derivatives of $\hat{\mathbf{A}}_{1,2}$, $\hat{\mathbf{A}}_{2,1}$, Y and C with respect to x_3, leads to

$$-\partial_3^2(C^{-1}(\hat{\mathbf{A}}'_{1,2})^{-1}\hat{\mathbf{f}}_1) + s\,\partial_3(C^{-1}\{(\hat{\mathbf{A}}'_{1,2})^{-1}, C\}\hat{\mathbf{f}}_1) + s^2(C^{-1}\hat{\mathbf{A}}'_{2,1} - (\hat{\mathbf{A}}'_{1,2})^{-1}C)\,\hat{\mathbf{f}}_1 = 0. \tag{92}$$

Here, $\{.,.\}$ denotes the anti-commutator. Next, we neglect the first term on the left-hand side with respect to the remaining ones, which is motivated by the fact C is such that the last term is small for vertical propagation. With the substitution $\hat{\mathbf{f}}_1 = \hat{\mathbf{A}}_{1,2}\langle\hat{\mathbf{w}}_1\rangle$ ($\langle\cdots\rangle$ denotes the approximation, with $\langle\hat{\mathbf{w}}_2\rangle = 0$) the equation above resembles the classical parabolically approximated wave equation

$$\partial_3(C^{-1}\{(\hat{\mathbf{A}}'_{1,2})^{-1}, C\}\hat{\mathbf{A}}_{1,2}\langle\hat{\mathbf{w}}_1\rangle) + s\,(C^{-1}\hat{\mathbf{A}}'_{2,1}\hat{\mathbf{A}}_{1,2} - (\hat{\mathbf{A}}'_{1,2})^{-1}C\hat{\mathbf{A}}_{1,2})\,\langle\hat{\mathbf{w}}_1\rangle = 0. \tag{93}$$

6. The space-time elastodynamic Green's tensor in a homogeneous isotropic medium

In this section we determine some significant features of the space-time elastodynamic Green's tensor (particle velocity of the wave motion generated by a point force) in a homogeneous isotropic medium in the parabolic approximation. The jump conditions representing the action of the source in the notional sources of Eqs. (9)–(10) are assumed to survive the parabolic approximation. For the space-time domain evaluation of the scalar Green's function in the parabolic approximation, which we will use in the subsequent analysis, we refer the reader to a previous paper [6].

6.1. The exact case

For a point force with signature $a_i\delta(t)$ operative at the origin, the relevant particle velocity is given by [30–33]:

$$v_i = (\partial_t^2 \boldsymbol{G}_{ij})\,a_j, \tag{94}$$

where (see also Appendix B)

$$\boldsymbol{G}_{ij} = \boldsymbol{G}^{\mathrm{P}}_{ij} + \boldsymbol{G}^{\mathrm{S}}_{ij} = c_{\mathrm{S}}^{-2}\,\delta_{ij}G^{\mathrm{S}} + \mathcal{D}_i\mathcal{D}_j\,(G^{\mathrm{P}} - G^{\mathrm{S}}), \tag{95}$$

in which

$$G^{\mathrm{P,S}} = \frac{1}{4\pi\rho R} H(t - T_{\mathrm{P,S}}), \tag{96}$$

with

$$T_{\mathrm{P,S}} = R/c_{\mathrm{P,S}} \tag{97}$$

and $R = (x_j x_j)^{1/2}$. Here, $\mathcal{D}_j$ is defined through its Laplace-domain counterpart $\hat{\mathcal{D}}_j = D_j = -s^{-1}\partial_j$ and amounts to a spatial differentiation and a temporal integration in the space-time domain.

The near-field region

In the near-field region the P- and S-wave contributions are non-separable and have to be taken together. It is found that

$$\boldsymbol{G}_{ij} \to \left\{ \frac{1}{c_{\mathrm{S}}^2}\delta_{ij}\frac{1}{4\pi\rho R} + \left(\frac{1}{2c_{\mathrm{P}}^2} - \frac{1}{2c_{\mathrm{S}}^2}\right)\left(\delta_{ij} - \frac{x_i x_j}{R^2}\right)\frac{1}{4\pi\rho R} \right\} H(t), \tag{98}$$

as $R \to 0$. Equation (98) shows that the singularity at the source is of order $O(R^{-1})$ and is indicative for the asymptotic behavior as $t \gg T_{\mathrm{P,S}}$ [30, p.75].

The far-field region

In the far-field region the P- and S-wave constituents are markedly separated, and we have

$$\boldsymbol{G}^{\mathrm{P}}_{ij} = \left\{ \frac{1}{c_{\mathrm{P}}^2}\frac{x_i x_j}{R^2}\frac{1}{4\pi\rho R} + \mathrm{O}(t - T_{\mathrm{P}}) \right\} H(t - T_{\mathrm{P}}) \tag{99}$$

and

$$\boldsymbol{G}^{\mathrm{S}}_{ij} = \left\{ \frac{1}{c_{\mathrm{S}}^2}\left(\delta_{ij} - \frac{x_i x_j}{R^2}\right)\frac{1}{4\pi\rho R} + \mathrm{O}(t - T_{\mathrm{S}}) \right\} H(t - T_{\mathrm{S}}). \tag{100}$$

Eqs. (99)–(100) are indicative for the asymptotic ray solution [30, p.74].

6.2. The parabolic approximation

In the first-order parabolic approximation we carry out the replacements

$$\gamma_{\mathrm{P}} \to \gamma^I_{\mathrm{P}}, \qquad \gamma_{\mathrm{S}} \to \gamma^I_{\mathrm{S}}, \tag{101}$$

where γ^I_{P} and γ^I_{S} are given by Eq. (81), while γ^2_{P} and γ^2_{S} are left as they are. Next, the resulting expressions are transformed back to the space-time domain with the aid of the modified Cagniard method [8,30–32]. The correspondingly approximated space-time Green's tensor is then found as (see also Appendix B)

$$\boldsymbol{G}^I_{ij} = \boldsymbol{G}^{\mathrm{P},I}_{ij} + \boldsymbol{G}^{\mathrm{S},I}_{ij} = c_{\mathrm{S}}^{-2}\,\delta_{i3}\delta_{j3}\frac{1}{2}\left[G^{\mathrm{S},I}_0 + c_{\mathrm{S}}\mathrm{sgn}(x_3)\mathcal{D}_3 G^{\mathrm{S},I}\right] + c_{\mathrm{S}}^{-2}\,\delta_{i\mu}\delta_{j\mu}G^{\mathrm{S},I} + \mathcal{D}_i\mathcal{D}_j\,(G^{\mathrm{P},I} - G^{\mathrm{S},I}), \tag{102}$$

where the parabolically approximated scalar P-wave function is given by (see Ref. [6])

$$G^{\mathrm{P},I} = \begin{cases} \dfrac{1}{4\pi\rho c_{\mathrm{P}}[t^2 - (T^I_{\mathrm{P},0})^2]^{1/2}}\left[2H(t - T^I_{\mathrm{P},0}) - H(t - T^I_{\mathrm{P}})\right] & \text{if } r/|x_3| \geq \sqrt{2}, \\ \dfrac{1}{4\pi\rho c_{\mathrm{P}}[t^2 - (T^I_{\mathrm{P},0})^2]^{1/2}}H(t - T^I_{\mathrm{P}}) & \text{if } r/|x_3| < \sqrt{2}, \end{cases} \tag{103}$$

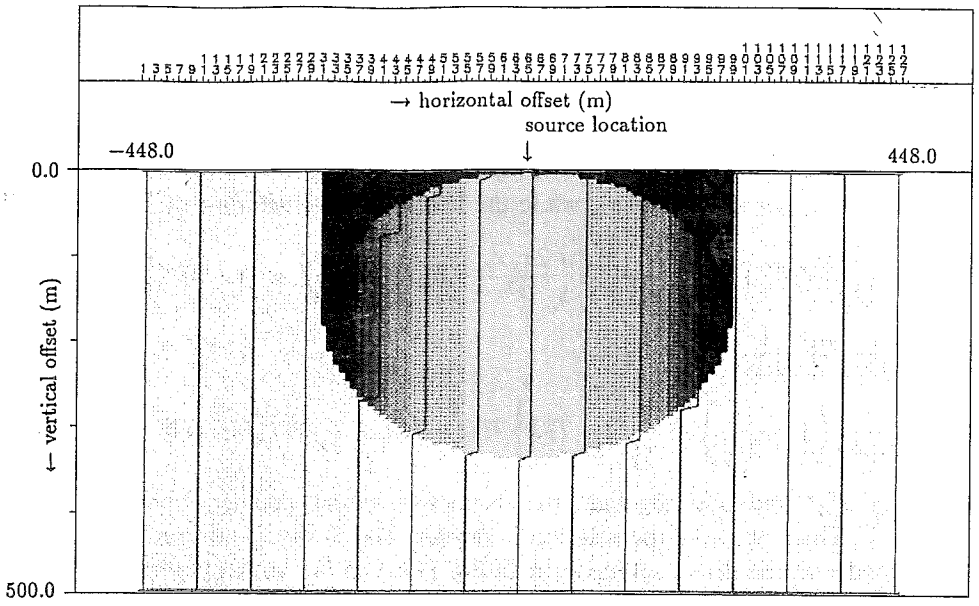

Fig. 5. Snapshot at $t = 0.450$ s of the parabolic scalar P-wave Green's function in space for $x_3 \geq 0$ with $c_P = 750$ m/s. (The horizontal offsets are numbered sequentially.)

with

$$T^I_{P,0} = \sqrt{2}\frac{r}{c_P}, \qquad T^I_P = \frac{|x_3|}{c_P}\left(1 + \frac{r^2}{2x_3^2}\right) \tag{104}$$

in which $r = (x_\mu x_\mu)^{1/2}$ is the horizontal distance from the source. This function is shown in Fig. 5. Note that $T^I_P > T^I_{P,0}$ when $r/|x_3| \neq \sqrt{2}$. A similar result holds for the parabolically approximated scalar S-wave function. Further,

$$G^{S,I}_0 = \frac{1}{8\pi\rho c_S[(t-\tau_0)^2 - (T_0-\tau_0)^2]^{1/2}} \begin{cases} [2H(t-T_0) - H(t-T^I_S)] & \text{if } r/|x_3| \geq 1, \\ H(t-T^I_S) & \text{if } r/|x_3| < 1, \end{cases} \tag{105}$$

with

$$\tau_0 = \frac{|x_3|}{2c_S}, \qquad T_0 = \frac{r}{c_S} + \tau_0, \qquad T^I_S = \frac{|x_3|}{c_S}\left(1 + \frac{r^2}{2x_3^2}\right). \tag{106}$$

The latter function is either found upon transforming the spectral-domain contribution

$$\begin{aligned} c_S^{-2}\frac{(\gamma^I_S)^2}{c_S^{-2} + \alpha_\kappa\alpha_\kappa}\hat{G}^{S,I} &= \frac{1}{2s^2\rho c_S^2}\frac{\gamma^I_S}{c_S^{-2} + \alpha_\kappa\alpha_\kappa}\exp(-s\gamma^I_S|x_3|) \\ &= \frac{1}{2}\left[\frac{1}{c_S + c_S^3\alpha_\kappa\alpha_\kappa} + \frac{1}{c_S}\right]\frac{1}{2s^2\rho}\exp(-s\gamma^I_S|x_3|) \end{aligned} \tag{107}$$

to the space–time domain with the aid of the modified Cagniard method (see Ref. [6]) or upon applying a proper scaling to Eq. (103).

The differentiations occurring in Eq. (102) are carried out in Appendix C. The P-wave contribution is then found as

$$G^{P,I}_{ij} = \mathcal{D}_i\mathcal{D}_j G^{P,I} + \delta_{i3}\delta_{j3}(2\rho)^{-1}\delta(x_1, x_2, x_3)t^2 H(t) = G^{P,H}_{ij} + G^{P,B}_{ij}, \tag{108}$$

where the artificial head-wave contribution is

$$G^{\mathrm{P},H}_{\mu\nu} = \frac{1}{4\pi\rho c_{\mathrm{P}}}\left\{\frac{2x_\mu x_\nu}{r^2}\frac{1}{c_{\mathrm{P}}^2}\frac{1}{[t^2-(T^I_{\mathrm{P},0})^2]^{1/2}} + \left(\frac{2x_\mu x_\nu}{r^2}-\delta_{\mu\nu}\right)\frac{1}{r^2}[t^2-(T^I_{\mathrm{P},0})^2]^{1/2}\right\}$$
$$\times\begin{cases}[2H(t-T^I_{\mathrm{P},0})-H(t-T^I_{\mathrm{P}})] & \text{if } r/|x_3|\geq\sqrt{2}\\ H(t-T^I_{\mathrm{P}}) & \text{if } r/|x_3|<\sqrt{2}\end{cases} \tag{109}$$

(the other elements of the tensor $G^{\mathrm{P},H}$ vanish), while the body-wave contribution is

$$G^{\mathrm{P},B}_{\mu\nu} = \frac{1}{4\pi\rho c_{\mathrm{P}}}\left\{-\frac{1}{2}\left(\frac{2x_\mu x_\nu}{r^2}+\delta_{\mu\nu}\right)\frac{1}{c_{\mathrm{P}}|x_3|} - \left(\frac{2x_\mu x_\nu}{r^2}-\delta_{\mu\nu}\right)\frac{1}{r^2}\left(\frac{|x_3|}{c_{\mathrm{P}}}+[t-T^I_{\mathrm{P}}]\right)\right\}H(t-T^I_{\mathrm{P}}), \tag{110}$$

$$G^{\mathrm{P},B}_{\mu 3} = G^{\mathrm{P},B}_{3\mu} = \frac{1}{4\pi\rho c_{\mathrm{P}}}\frac{x_\mu}{x_3}\frac{1}{c_{\mathrm{P}}|x_3|}H(t-T^I_{\mathrm{P}}), \tag{111}$$

$$G^{\mathrm{P},B}_{33} = \frac{1}{4\pi\rho c_{\mathrm{P}}}\left\{\frac{1}{c_{\mathrm{P}}|x_3|}\left(1-\frac{r^2}{2x_3^2}\right)+\frac{1}{x_3^2}[t-T^I_{\mathrm{P}}]\right\}H(t-T^I_{\mathrm{P}}) + \frac{1}{2\rho}\delta(x_1,x_2,x_3)t^2H(t). \tag{112}$$

Note that upon taking $G^{\mathrm{P},H}_{\mu\nu}$ and $G^{\mathrm{P},B}_{\mu\nu}$ together, the factor r^{-2} in the second terms vanishes in the Taylor expansion about $t = T^I_{\mathrm{P}}$. Thus, at $r = 0$ the solution is regular. The S-wave contribution follows along similar lines. Further, it is noted that the direct source term in Eq. (112) is the same for P and S waves. Hence, this term vanishes in expression Eq. (102).

Finally, it follows that

$$\mathrm{sgn}(x_3)\mathcal{D}_3 G^{\mathrm{S},I} = \frac{1}{4\pi\rho c_{\mathrm{S}}|x_3|}H(t-T^I_{\mathrm{S}}). \tag{113}$$

This completes the evaluation of the right-hand side of Eq. (102).

The near-field region

Just as in the exact case, the P- and S-wave near-field ($t \gg T^I_{\mathrm{P,S}}$) contributions in the parabolic approximation are not separated and have to be taken together. It is found that several cancellations occur. The result is

$$G^I_{\mu\nu} \to -\left(\frac{1}{c_{\mathrm{P}}^2}-\frac{1}{c_{\mathrm{S}}^2}\right)\delta_{\mu\nu}\frac{1}{4\pi\rho|x_3|}H(t), \tag{114}$$

$$G^I_{\mu 3}, G^I_{3\mu} \to \left(\frac{1}{c_{\mathrm{P}}^2}-\frac{1}{c_{\mathrm{S}}^2}\right)\frac{x_\mu}{x_3}\frac{1}{4\pi\rho|x_3|}H(t), \tag{115}$$

$$G^I_{33} \to \left(\frac{1}{c_{\mathrm{P}}}-\frac{1}{c_{\mathrm{S}}}\right)\frac{1}{4\pi\rho|x_3|}\frac{t}{|x_3|}H(t), \tag{116}$$

which determines the order of the singularities in the limits $r \to 0$ and $x_3 \to 0$. The differences as compared with the exact expression (cf. Eq. (98)) are noteworthy.

The far-field region

In the far-field region ($t \to T^I_{\mathrm{P}}$, or $t \to T^I_{\mathrm{S}}$) the P- and S-wave constituents can, again, be separated. In the neighborhood of their body-wave fronts the P-wave contribution is found as

$$G^{\mathrm{P},I}_{\mu\nu} = \left\{\frac{1}{c_{\mathrm{P}}^2}\frac{x_\mu x_\nu}{x_3^2}\frac{1}{4\pi\rho|x_3|}\left(1-\frac{r^2}{2x_3^2}\right)^{-1}+\mathrm{O}(t-T^I_{\mathrm{P}})\right\}H(t-T^I_{\mathrm{P}}), \tag{117}$$

$$G^{\mathrm{P},I}_{\mu 3} = G^{\mathrm{P},I}_{3\mu} = \frac{1}{c_{\mathrm{P}}^2}\frac{x_\mu}{x_3}\frac{1}{4\pi\rho|x_3|}H(t-T^I_{\mathrm{P}}), \tag{118}$$

$$G^{\mathrm{P},I}_{33} = \left\{\frac{1}{c_{\mathrm{P}}^2}\frac{1}{4\pi\rho|x_3|}\left(1-\frac{r^2}{2x_3^2}\right)+\mathrm{O}(t-T^I_{\mathrm{P}})\right\}H(t-T^I_{\mathrm{P}}), \tag{119}$$

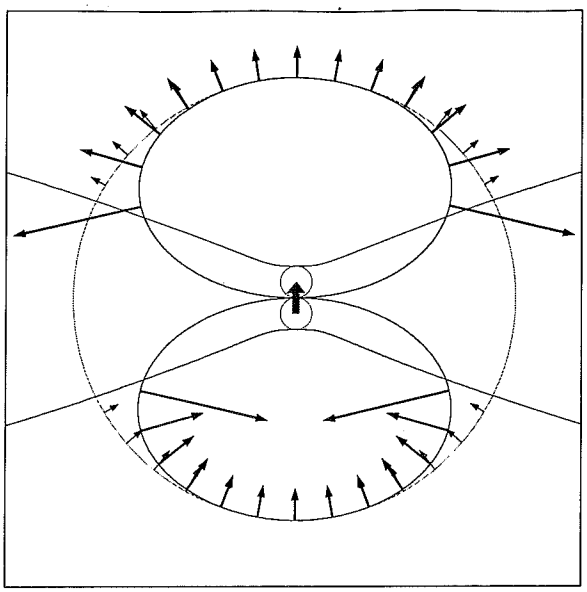

Fig. 6. The far-field radiation pattern for P waves due to a vertical point force (in the plane $x_2 = 0$). The sphere corresponds with the exact pattern and the double oblate spheroid corresponds with its parabolic approximation.

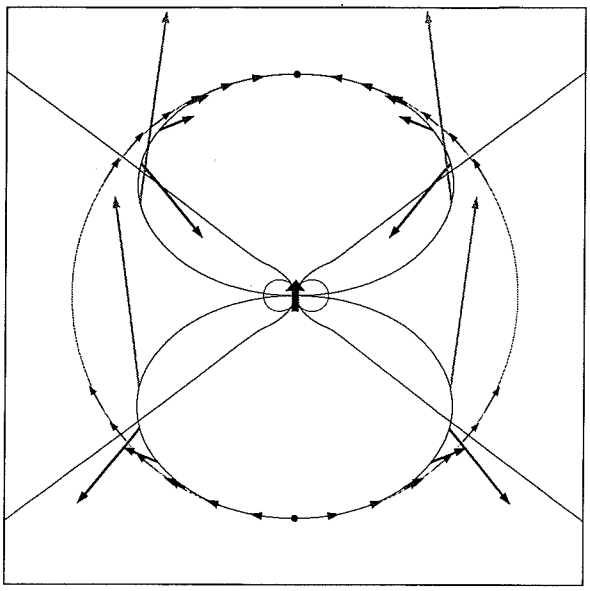

Fig. 7. The far-field radiation pattern for S waves due to a vertical point force (in the plane $x_2 = 0$). The shaded arrows should be multiplied by 5. The sphere corresponds with the exact pattern and the double oblate spheroid corresponds with its parabolic approximation.

while the S-wave contribution is

$$\boldsymbol{G}^{\mathrm{S},I}_{\mu\nu} = \left\{ \frac{1}{c_{\mathrm{S}}^2}\left(\delta_{\mu\nu} - \frac{x_\mu x_\nu}{x_3^2}\right)\frac{1}{4\pi\rho|x_3|}\left(1 - \frac{r^2}{2x_3^2}\right)^{-1} + \mathrm{O}(t - T^I_{\mathrm{S}})\right\} H(t - T^I_{\mathrm{S}}), \tag{120}$$

$$\boldsymbol{G}^{\mathrm{S},I}_{\mu 3} = \boldsymbol{G}^{\mathrm{S},I}_{3\mu} = -\frac{1}{c_{\mathrm{S}}^2}\frac{x_\mu}{x_3}\frac{1}{4\pi\rho|x_3|} H(t - T^I_{\mathrm{S}}), \tag{121}$$

$$\boldsymbol{G}^{\mathrm{S},I}_{33} = \left\{ \frac{1}{c_{\mathrm{S}}^2}\frac{r^2}{x_3^2}\left(1 - \frac{r^2}{x_3^2}\right)^{-1}\frac{1}{4\pi\rho|x_3|}\left(1 - \frac{r^2}{2x_3^2}\right) + \mathrm{O}(t - T^I_{\mathrm{S}})\right\} H(t - T^I_{\mathrm{S}}). \tag{122}$$

To obtain the latter results, the following estimates were used:

$$G^{\mathrm{S},I} = \left\{ \frac{1}{4\pi\rho|x_3|}\left(1 - \frac{r^2}{2x_3^2}\right)^{-1} + \mathrm{O}(t - T^I_{\mathrm{S}})\right\} H(t - T^I_{\mathrm{S}}), \tag{123}$$

$$G^{\mathrm{S},I}_0 = \left\{ \frac{1}{4\pi\rho|x_3|}\left(1 - \frac{r^2}{x_3^2}\right)^{-1} + \mathrm{O}(t - T^I_{\mathrm{S}})\right\} H(t - T^I_{\mathrm{S}}), \tag{124}$$

$$c_{\mathrm{S}}\mathrm{sgn}(x_3)\mathcal{D}_3 G^{\mathrm{S},I} = \frac{1}{4\pi\rho|x_3|} H(t - T^I_{\mathrm{S}}). \tag{125}$$

The corresponding radiation patterns are shown in Figs. 6 to 9. (For the exact expressions Fig. 8 is obtained from Fig. 6 by a rotation over $\pi/2$; likewise Fig. 9 is obtained from Fig. 7 by a rotation over $\pi/2$; in the parabolic approximation this is no longer true.) Accurate results are obtained in a cone centered on the vertical axis. The head-wave-like arrivals were not considered; they follow from a different expansion, viz., the one about $t = T^I_{\mathrm{P},0}$ or about $t = T^I_{\mathrm{S},0}$.

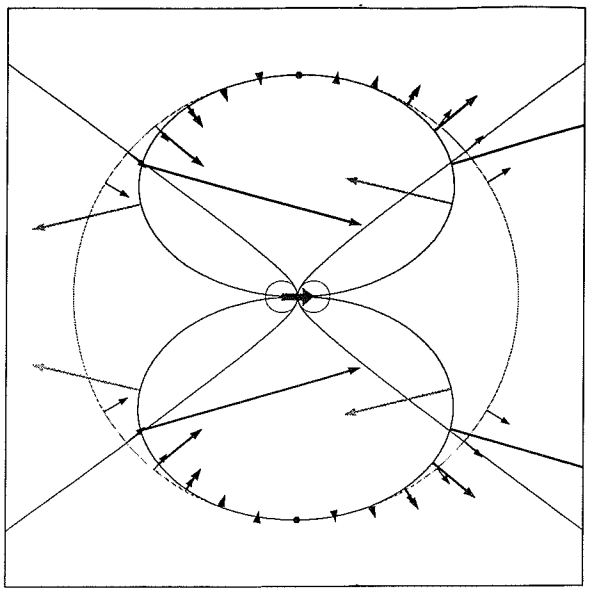

Fig. 8. The far-field radiation pattern for P waves due to a horizontal point force (in the plane $x_2 = 0$). The shaded arrows should be multiplied by 5. The sphere corresponds with the exact pattern and the double oblate spheroid corresponds with its parabolic approximation.

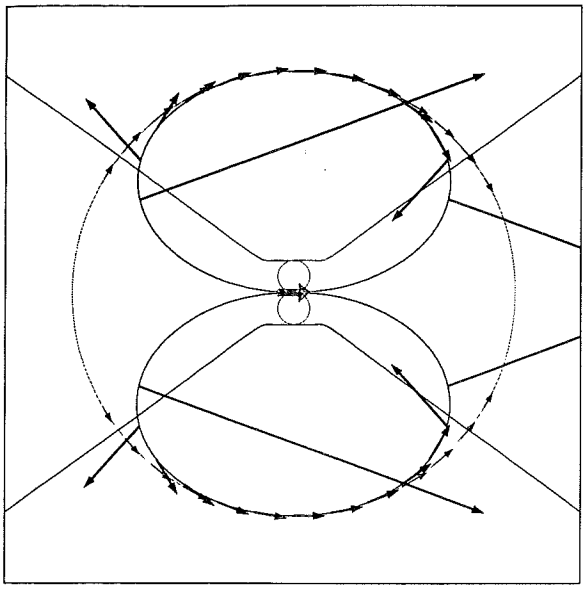

Fig. 9. The far-field radiation pattern for S waves due to a horizontal point force (in the plane $x_2 = 0$). The sphere corresponds with the exact pattern and the double oblate spheroid corresponds with its parabolic approximation.

7. Discussion of the results

Through an appropriate two-level operator approach a consistent scheme for the up/down decomposition of elastic wave fields in inhomogeneous and anisotropic media, and their subsequent decomposition into polarization states has been developed. The procedure has been worked out in detail for the class of orthorhombic media and lateral variations are taken into account. The high-frequency approximation to the operator approach is shown to be amenable to matrix manipulation in the conventional horizontal Fourier transform domain. The hexagonal (TIV) and the isotropic case are discussed as examples. Finally, the space–time peculiarities and artifacts of the corresponding two-level parabolic approximation to the particle velocity of the elastic wave motion generated by a point force in a homogeneous, isotropic solid have been discussed in detail.

In the context of migration, it is conjectured that the downward continuation part should be carried out prior to separating the polarization states, but that with a view to inverse scattering it would be attractive to do the separation just before imaging to generate sections for the different mode conversions. An accurate wave speed model is still a prerequisite; such a model can, in principle, be obtained from the arrival times of the individual polarization constituents using traveltime inversion.

Acknowledgement

The authors would like to thank Drs. R.L.J.P. Fonk, Koninklijke/Shell Exploratie en Produktie Laboratorium, and Dr. C. Spencer, Schlumberger Cambridge Research, for their help to produce the figures.

Appendix A. Approximations of the vertical slownesses in a TIV medium

In the example of a TIV medium, we employed the following schemes to approximate the principal symbols γ and γ^2. The azimuthal isotropy is exploited through the notation

$$\alpha = (\alpha_1^2 + \alpha_2^2)^{1/2}, \quad \gamma(\alpha^2) = \gamma(\mathrm{i}\alpha, 0). \tag{A.1}$$

The Lagrange *polynomial* interpolation of a branch $\gamma(\alpha^2)$ of the slowness surface through the points $\{\alpha_0^2, \alpha_1^2, \alpha_2^2, \cdots\}$ is given by

$$\gamma^{(p)}(\alpha^2) = \sum_k v_k(\alpha^2)\,\gamma(\alpha_j^2), \tag{A.2}$$

with

$$v_k(\alpha^2) = \frac{\prod_{i\neq k}(\alpha^2 - \alpha_i^2)}{\prod_{i\neq k}(\alpha_k^2 - \alpha_i^2)}. \tag{A.3}$$

The Newton *continued-fraction* interpolation of a branch $\gamma(\alpha^2)$ through the points $\{\alpha_0^2, \alpha_1^2, \alpha_2^2, \cdots\}$ is given by

$$\gamma^{(p)}(\alpha^2) = a_0 + \cfrac{\alpha^2 - \alpha_0^2}{a_1 + \cfrac{\alpha^2 - \alpha_1^2}{a_2 + \cfrac{\alpha^2 - \alpha_2^2}{a_3 + \cdots}}} \tag{A.4}$$

with coefficients $a_k = v_k(\alpha_k^2)$, where

$$v_0(\alpha^2) = \gamma(\alpha^2), \quad v_{k+1}(\alpha^2) = \frac{\alpha^2 - \alpha_k^2}{v_k(\alpha^2) - v_k(\alpha_k^2)}. \tag{A.5}$$

From these expressions similar approximations can be obtained for the squared vertical slownesses.

Appendix B. The transform-domain particle velocity in an unbounded homogeneous isotropic solid due to a point force

In the spectral domain, the acoustic wave field generated by a point force located at $x_1 = x_2 = x_3 = 0$ in an unbounded homogeneous isotropic solid, can be written as the superposition of its eigenmodes through Eqs. (60)–(61)). The procedure is standard, but, in view of the parabolic approximation, we have to take care to treat γ_P, γ_S and their squares independently.

The spectral-domain elastodynamic Green's tensor decomposes into a P-wave part and an S-wave part according to (cf. Eq. (17))

$$\tilde{v}_i = s^2(\tilde{G}_{ij}^{P} + \tilde{G}_{ij}^{S})\,a_j, \tag{B.1}$$

where the P-wave part is found as

$$\tilde{G}^{P} = \begin{pmatrix} -\alpha_1^2 & -\alpha_1\alpha_2 & \mathrm{i}\alpha_1 \mathrm{sgn}(x_3)\gamma_P \dfrac{2\chi - \alpha_\rho\alpha_\rho}{c_S^{-2} + \alpha_\kappa\alpha_\kappa} \\ -\alpha_1\alpha_2 & -\alpha_2^2 & \mathrm{i}\alpha_2 \mathrm{sgn}(x_3)\gamma_P \dfrac{2\chi - \alpha_\rho\alpha_\rho}{c_S^{-2} + \alpha_\kappa\alpha_\kappa} \\ \mathrm{i}\alpha_1 \mathrm{sgn}(x_3)\gamma_P & \mathrm{i}\alpha_2 \mathrm{sgn}(x_3)\gamma_P & \gamma_P\gamma_P \dfrac{2\chi - \alpha_\rho\alpha_\rho}{c_S^{-2} + \alpha_\kappa\alpha_\kappa} \end{pmatrix} \tilde{G}^{P}, \tag{B.2}$$

with

$$\tilde{G}^{\mathrm{P}} = \frac{1}{2s^2\rho\gamma_{\mathrm{P}}}\exp(-s\gamma_{\mathrm{P}}|x_3|) \tag{B.3}$$

and the S-wave part is found as

$$\tilde{G}^{\mathrm{S}} = \left\{ \begin{pmatrix} c_{\mathrm{S}}^{-2} & 0 & 0 \\ 0 & c_{\mathrm{S}}^{-2} & 0 \\ 0 & 0 & c_{\mathrm{S}}^{-2}\dfrac{\gamma_{\mathrm{S}}\gamma_{\mathrm{S}}}{c_{\mathrm{S}}^{-2}+\alpha_\kappa\alpha_\kappa} \end{pmatrix} - \begin{pmatrix} -\alpha_1^2 & -\alpha_1\alpha_2 & \mathrm{i}\alpha_1\mathrm{sgn}(x_3)\gamma_{\mathrm{S}}\dfrac{2\chi-\alpha_\rho\alpha_\rho}{c_{\mathrm{S}}^{-2}+\alpha_\kappa\alpha_\kappa} \\ -\alpha_1\alpha_2 & -\alpha_2^2 & \mathrm{i}\alpha_2\mathrm{sgn}(x_3)\gamma_{\mathrm{S}}\dfrac{2\chi-\alpha_\rho\alpha_\rho}{c_{\mathrm{S}}^{-2}+\alpha_\kappa\alpha_\kappa} \\ \mathrm{i}\alpha_1\mathrm{sgn}(x_3)\gamma_{\mathrm{S}} & \mathrm{i}\alpha_2\mathrm{sgn}(x_3)\gamma_{\mathrm{S}} & \gamma_{\mathrm{S}}\gamma_{\mathrm{S}} \end{pmatrix} \right\} \tilde{G}^{\mathrm{S}}, \tag{B.4}$$

with

$$\tilde{G}^{\mathrm{S}} = \frac{1}{2s^2\rho\gamma_{\mathrm{S}}}\exp(-s\gamma_{\mathrm{S}}|x_3|). \tag{B.5}$$

In the exact expression, $\gamma_{\mathrm{P}}, \gamma_{\mathrm{S}}$ and χ retain their exact values as given by Eqs. (76)–(75) and Eq. (77); in the parabolic approximation, γ_{P} and γ_{S} are replaced by their approximate values as given by Eq. (81). As Eqs. (B.1)–(B.5) show, the elastodynamic Green's tensor can be expressed in terms of the Green's function of the scalar wave equation under the application of the standard differentiation and integration rules of the one-sided time Laplace transformation and the spatial Fourier transformation. The latter property applies to the exact expression as well as to the parabolic approximation.

Appendix C. Evaluation of the first-order approximated elastodynamic Green's tensor

In the space–time equivalent of the parabolically approximated Green's tensor functions of the type

$$\mathcal{G} = \frac{1}{[t^2 - T_1^2]^{1/2}} H(t - T_2) \tag{C.1}$$

occur, where T_1 and T_2 are functions of x_j, with $T_1 \leq T_2$. The operator $\mathcal{D}_j$ has been defined through $\hat{\mathcal{D}}_j = -s^{-1}\partial_j$, where s is the time-Laplace-transform parameter. We will evaluate $\mathcal{D}_j\mathcal{G}$ and $\mathcal{D}_i\mathcal{D}_j\mathcal{G}$.

First consider the case where $T_1 < T_2$. Then, in the distributional sense, it is found that

$$\mathcal{D}_j\mathcal{G} = \frac{(\partial_j T_1)}{T_1}\frac{t}{[t^2 - T_1^2]^{1/2}} H(t - T_2) + \frac{T_1(\partial_j T_2) - T_2(\partial_j T_1)}{T_1[T_2^2 - T_1^2]^{1/2}} H(t - T_2). \tag{C.2}$$

If $T_2 = T_1$, $\mathcal{D}_j\mathcal{G}$ follows from the diagram

$$\begin{array}{ccc} \dfrac{1}{[t^2 - T_1^2]^{1/2}} H(t - T_1) & \xrightarrow{\mathcal{D}_j} & \dfrac{(\partial_j T_1)}{T_1}\dfrac{t}{[t^2 - T_1^2]^{1/2}} H(t - T_1) \\ \downarrow\mathcal{L} & & \downarrow\mathcal{L} \\ K_0(sT_1) & \xrightarrow{-s^{-1}\partial_j} & (\partial_j T_1) K_1(sT_1) \end{array} \tag{C.3}$$

where K_0 and K_1 are the modified Bessel functions of the second kind and orders zero and one, respectively, and $\mathcal{L}$ denotes the Laplace transformation with respect to time.

The second-order derivatives are found as

$$\mathcal{D}_i\mathcal{D}_j\mathcal{G} = (\partial_i T_1)(\partial_j T_1)\frac{1}{[t^2 - T_1^2]^{1/2}} H(t - T_2) + \frac{(\partial_i T_1)(\partial_j T_1) - T_1(\partial_i\partial_j T_1)}{T_1^2}[t^2 - T_1^2]^{1/2} H(t - T_2)$$
$$- \frac{(\partial_j T_1)(\partial_i T_1) - (\partial_i T_2)(\partial_j T_2)}{[T_2^2 - T_1^2]^{1/2}} H(t - T_2) - \frac{(\partial_i T_1)(\partial_j T_1) - T_1(\partial_i\partial_j T_1)}{T_1^2}[T_2^2 - T_1^2]^{1/2} H(t - T_2)$$
$$+ \left\{ \frac{(2T_1^2 - T_2^2)T_2(\partial_i T_1)(\partial_j T_1)}{T_1^2[T_2^2 - T_1^2]^{3/2}} - \frac{T_1^3[(\partial_i T_1)(\partial_j T_2) + (\partial_i T_2)(\partial_j T_1)] - T_1^2 T_2(\partial_i T_2)(\partial_j T_2)}{T_1^2[T_2^2 - T_1^2]^{3/2}} \right.$$
$$\left. + \frac{T_2(\partial_i\partial_j T_1) - T_1(\partial_i\partial_j T_2)}{T_1[T_2^2 - T_1^2]^{1/2}} \right\} (t - T_2) H(t - T_2) \tag{C.4}$$

if $T_1 < T_2$. In the case $T_2 = T_1$, we employ the diagram:

$$\begin{array}{ccc} \dfrac{(\partial_j T_1)}{T_1}\dfrac{t}{[t^2 - T_1^2]^{1/2}} H(t - T_1) & \xrightarrow{\mathcal{D}_i} & (\partial_i T_1)(\partial_j T_1)\dfrac{1}{[t^2 - T_1^2]^{1/2}} H(t - T_1) \\ & & + \dfrac{(\partial_i T_1)(\partial_j T_1) - T_1(\partial_i\partial_j T_1)}{T_1^2}[t^2 - T_1^2]^{1/2} H(t - T_1) \\ \downarrow \mathcal{L} & & \downarrow \mathcal{L} \\ (\partial_j T_1) K_1(sT_1) & \xrightarrow{-s^{-1}\partial_i} & (\partial_i T_1)(\partial_j T_1) K_0(sT_1) \\ & & + \dfrac{(\partial_i T_1)(\partial_j T_1) - T_1(\partial_i\partial_j T_1)}{T_1}\dfrac{K_1(sT_1)}{s} \end{array} \tag{C.5}$$

So far, we used the equalities $K_0'(z) = -K_1(z)$ and $K_1'(z) = -z^{-1}K_1(z) - K_0(z)$.

In our application, we have

$$T_1 = \sqrt{2}\frac{r}{c}, \quad T_2 = \frac{|x_3|}{c}\left(1 + \frac{r^2}{2x_3^2}\right), \tag{C.6}$$

with $c = c_P, c_S$, and $r = (x_\mu x_\mu)^{1/2}$. Note that $T_2 > T_1$ when $r/|x_3| \neq \sqrt{2}$; only for $r/|x_3| = \sqrt{2}$ we have $T_2 = T_1$. From Eq. (C.6), it follows that

$$\partial_1 T_1 = \frac{\sqrt{2}}{c}\frac{x_1}{r}, \quad \partial_2 T_1 = \frac{\sqrt{2}}{c}\frac{x_2}{r}, \quad \partial_3 T_1 = 0 \tag{C.7}$$

and

$$\partial_1 T_2 = \frac{1}{c}\frac{x_1}{|x_3|}, \quad \partial_2 T_2 = \frac{1}{c}\frac{x_2}{|x_3|}, \quad \operatorname{sgn}(x_3)\,\partial_3 T_2 = \frac{1}{c}\left(1 - \frac{r^2}{2x_3^2}\right), \tag{C.8}$$

while

$$\partial_1\partial_2 T_1 = -\frac{\sqrt{2}}{rc}\frac{x_1 x_2}{r^2}, \quad \partial_1^2 T_1 = \frac{\sqrt{2}}{rc}\left(1 - \frac{x_1^2}{r^2}\right), \quad \partial_2^2 T_1 = \frac{\sqrt{2}}{rc}\left(1 - \frac{x_2^2}{r^2}\right), \quad \partial_3^2 T_1 = 0 \tag{C.9}$$

which diverge as $r \downarrow 0$, and

$$\partial_1\partial_2 T_2 = 0, \quad \partial_1^2 T_2 = \partial_2^2 T_2 = \frac{1}{c}\frac{1}{|x_3|}, \quad \partial_3^2 T_2 = \frac{1}{c}\frac{r^2}{|x_3|^3}. \tag{C.10}$$

Further,

$$[T_2^2 - T_1^2]^{1/2} = \frac{|x_3|}{c}\left|1 - \frac{r^2}{2x_3^2}\right|. \tag{C.11}$$

The latter equations have to be substituted into Eqs. (C.4)–(refeq:3.A.5).

References

[1] A.T. de Hoop and H.J. Stam, "Time-domain reciprocity theorems for elastodynamic wave fields in solids with relaxation and their application to inverse problems," *Wave Motion 10*, 479–489 (1988).
[2] J.F. Claerbout, "Coarse grid calculations of waves in inhomogeneous media with application to delineation of complicated seismic structure", *Geoph. 35*, 407–418 (1970).
[3] P.W. Kitchenside, "2-D anisotropic migration in the space–frequency domain", *J. Seismic Exploration 2*, 7–22 (1993).
[4] M.V. de Hoop, *Directional decomposition of transient acoustic wave fields*, Delft University Press, Delft (1992).
[5] R.T. Coates and C.H. Chapman, "Generalized Born scattering of elastic waves in 3-D media", *Geophys. J. Int. 107*, 231–263 (1991).
[6] M.V. de Hoop and A.T. de Hoop, "Scalar space–time waves in their spectral domain first- and second-order Thiele approximations", *Wave Motion 15*, 229–265 (1992).
[7] M.V. de Hoop and A.T. de Hoop, "Interface reflection of spherical acoustic waves in the first- and second-order rational parabolic approximations and their artifacts", *J. Acoust. Soc. Am. 93*, 22–35 (1993).
[8] A.T. de Hoop, "A modification of Cagniard's method for solving seismic pulse problems", *Appl. Sci. Res. B8*, 349–356 (1960).
[9] J.H.M.T. van der Hijden, *Propagation of transient elastic waves in stratified anisotropic media*, North-Holland, Amsterdam (1987).
[10] J.A. Hudson, "A parabolic approximation for elastic waves", *Wave Motion 2*, 207–214 (1980).
[11] J.A. Hudson, "A parabolic approximation for surface waves", *Geophys. J. Roy. Astron. Soc. 67*, 755–770 (1981).
[12] A.J. Haines, "A phase-front method – I. Narrow-frequency-band SH waves", *Geophys. J. Roy. Astron. Soc. 72*, 783–808 (1983).
[13] T. Landers and J.F. Claerbout, "Numerical calculations of elastic waves in laterally inhomogeneous media", *J. Geophys. Res. 77*, 1476–1482 (1972).
[14] J.J. McCoy, "A parabolic theory of stress wave propagation through inhomogeneous linearly elastic solids", *J. Appl. Mech. 44*, 462–468 (1977).
[15] S.C. Wales and J.J. McCoy, "A comparison of parabolic wave theories for linearly elastic solids", *Wave Motion 5*, 99–113 (1983).
[16] S.C. Wales, "A vector parabolic equation model for elastic propagation", in *Ocean seismo-acoustics, proceedings of a SACLANT ASW Research Center Symposium La Spezia*, eds. T. Akal and J.M. Berkson, pp. 57–66, Plenum Press, New York (1986).
[17] C.P.A. Wapenaar and A.J. Berkhout, *Elastic wave field extrapolation*, Elsevier, Amsterdam (1989).
[18] J.P. Corones, B. DeFacio and R.J. Krueger, "Parabolic approximations to the time-dependent elastic wave equation", *J. Math. Phys. 23*, 577–586 (1982).
[19] C.P.A. Wapenaar, G.C. Haimé and A.J. Berkhout, "Elastic wavefield decomposition: before or after extrapolation?", 61st Ann. Internat. Mtg. Soc. Expl. Geophys., *Expanded Abstracts*, 1001–1004 (1991).
[20] M.D. Collins, "Higher-order and elastic parabolic equations for wave propagation in the ocean", in *Computational Acoustics Vol.3*, pp. 167–184, North-Holland, Amsterdam (1990).
[21] B. Wetton and G. Brooke, "One-way seismo-acoustic propagation in elastic waveguides with range-dependent material parameters", in *Computational Acoustics Vol. 3*, pp. 275–288, North-Holland, Amsterdam (1990).
[22] M.J.P. Musgrave, *Crystal Acoustics*, Holden Day, San Francisco (1970).
[23] B.A. Auld, *Acoustic Fields and Waves in Solids*, Wiley, New York (1973).
[24] C. Thomson, T. Clarke and J. Garmany, "Observations on seismic wave equation and reflection coefficient symmetries in stratified media", *Geophys. J. Roy. Astron. Soc. 86*, pp. 675–686 (1986).
[25] M.A. Shubin, *Pseudodifferential Operators and Spectral Theory*, Springer, Berlin (1987).
[26] M. Schoenberg and J. Protazio, " 'Zoeppritz' rationalized and generalized to anisotropy", *J. Seismic Exploration 1*, pp. 125–144 (1992).
[27] F.B. Hildebrand, *Introduction to Numerical Analysis*, McGraw-Hill, New York (1956).
[28] K. Helbig and M. Schoenberg, "Anomalous polarization of elastic waves in transversely isotropic media", *J. Acoust. Soc. Am. 81*, 1235–1245 (1987).
[29] R.G. Payton, *Elastic Wave Propagation In Transversely Anisotropic Media*, Martinus Nijhoff, The Hague (1983).
[30] K. Aki and P.G. Richards, *Quantitative Seismology*, Freeman, San Francisco (1980).
[31] J.D. Achenbach, *Wave Propagation In Elastic Solids*, North-Holland, Amsterdam (1973).
[32] J. Miklowitz, *The Theory of Elastic Waves and Wave Guides*, North-Holland, Amsterdam (1978).
[33] A.E.H. Love, *A Treatise on the Mathematical Theory of Elasticity*, 4th ed., Cambridge University Press, Cambridge (1959).